

*Fermi National Accelerator Laboratory*  
*Particle Physics Division*

Mechanical Department Engineering Note

**Number:** *MD-Eng-134*

**Date:** *19 October 2007*

**Project:** *DES*

**Project Internal Reference:** *DES DocDB 979*

**Title:** ***Mechanical Design of the  
DES V2.1 2k x 4k CCD Module***

**Author(s):** *Greg Derylo ([derylo@fnal.gov](mailto:derylo@fnal.gov)) FNAL/PPD/MD*

**Reviewer(s):** *---*

**Key Words:** *DES / CCD*

**Abstract/Summary:**

The updated design of the 2k x 4k pedestal-style module is presented. The assembly process is outlined and the manpower needed is estimated for a production rate of five modules per week. The results of FEA analyses are reported and found a  $\sim 3^{\circ}\text{C}$  gradient through the module and  $\sim 3.5$  microns of thermal distortion. Module mating with a revised focal plane support plate design is discussed; including pin fit determination, module-to-module gap control, and spring load determination. An installation process concept is also presented.

**Applicable Codes:** *N/A*

## **1.0 INTRODUCTION**

The V1 design of this module was based on previous work with these CCDs by LBNL and UCSC/Lick [Refs 1-3]. Several V1 devices were constructed and tested at FNAL [Ref 4] and several items were identified as desired changes for the V2 design (Ref 5):

1. Investigate moving some electrical components (JFETS etc.) to the AIN board.
2. Evaluate use of an alternate connector type and investigate allowing permanent attachment of the readout cable to reduce connector handling. This would have implications on module handling, storage, testing, and installation.
3. Redesign modules to allow wirebonding on the completed package rather than partway through assembly. This would reduce the number of CCD handling steps during assembly and would potentially allow damaged wirebonds to be repaired on completed modules.
4. Revise assembly techniques to eliminate the small tape pieces used during assembly that appear in CCD images.
5. Optimize module interface design with focal plane support plate.

However, before the V2 effort got underway, it was desired to build some additional modules for testing the first two items on this list. These modules were designated as V2.0 packages. Since a new foot was required anyway for the wider Hirose connector, it was designed with deep access manual wirebonding in mind in order to allow testing of this concept. One module with this foot design (# T1-02) was bonded with the K&S 4523D bonder at FCC and subsequent testing verified module functionality. The V1 and V2.0 modules are shown in Figure 1.0-1.

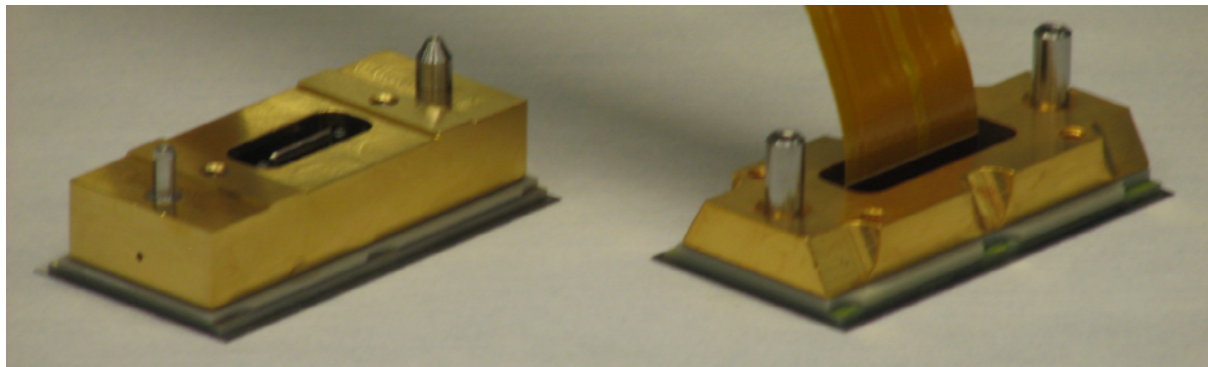


**Figure 1.0-1:** Photo of V1 and V2.0 Modules

Using the lessons from V1 and V2.0, the V2.1 module design (Figure 1.0-2) is being developed and is being documented in this report. The new design preserves the four layers of the previous design – CCD, AIN readout board, AIN spacer, and Invar mounting foot, as well as two different mounting pins. The mounting is different from V1 and is discussed in greater detail below.

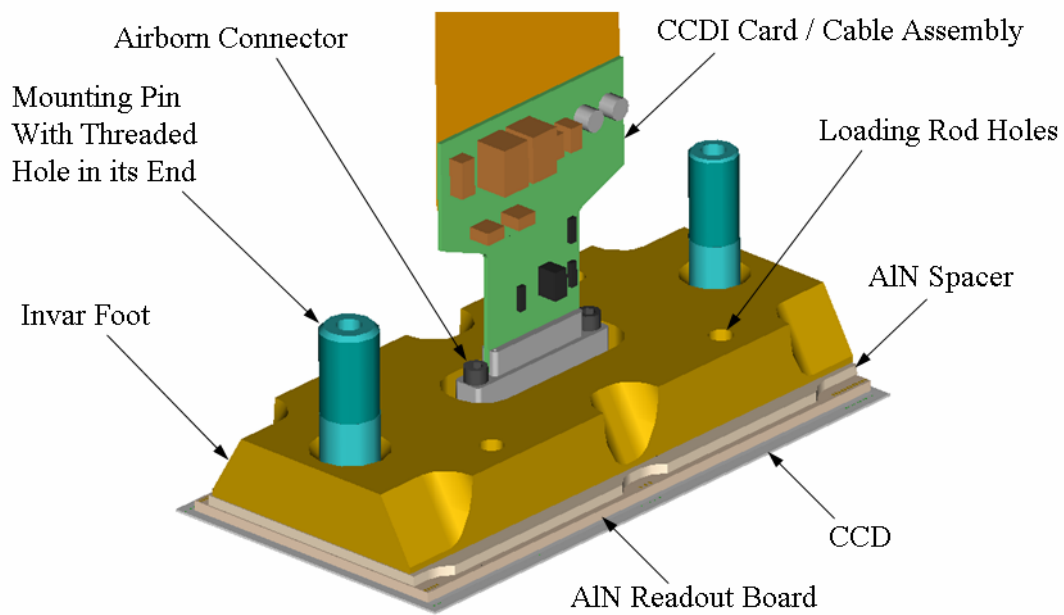


**Figure 1.0-2:** Image of the V2.1 Module Design

This report documents several aspects of the module design. An index is provided below:

Section	Description	Page
1.0	Introduction	2
2.0	Evaluation	4
2.1	Elements of the Module Design	4
2.2	Module Assembly	7
2.3	Module Thermal Analysis	10
2.4	Module Thermal Deformation & Stress Analysis	11
2.5	Module Flatness Considerations	16
2.6	Module / FPSP Interface	17
2.7	Module Storage Box	32
3.0	Conclusion	32
4.0	References	33

## **2.0 EVALUATION**

The drawing numbers for the assemblies and parts are listed below. Also included are drawings related to mounting to the focal plane support plate (FPSP). In addition to the FNAL drawing library, drawing copies can also be found in DES DocDB #979.

<u>Description</u>	<u>Drawing</u>
V2.1 Module Assembly	436408
2k x 4k CCD	436006
V2.1 Foot Subassembly	436409
V2.1 Readout Board	436410
V2.1 AlN Spacer	436411
V2.1 Foot	435412
V2.1 Mounting Pin (5mm)	436413
V2.1 Mounting Pin (6mm)	436414
V2.1 Module / FPSP Interface	436406
V2.1 FPSP Sample Section	436407
V2.1 CCDI Card/Cable Assembly	436415
V2.1 Module Mounting Screw	436416
V2.1 Cable Restraint Plate	436417
V2.1 Handling Rod	436418

Various aspects of the module design are discussed further in the sections below.

### **2.1 ELEMENTS OF THE MODULE DESIGN**

A brief discussion of each of the items in the module is included below.

CCD – The sensor is unchanged from the previous module versions.

AlN Readout Board – The size and thickness of the board is unchanged from V1, but it has two differences. The first is that the Nanonics connector is being replaced by a very similar connector made by Airborn. The main mechanical benefit from this change is that the mating screws are larger (#0-80's rather than M1.2's), thus allowing use of a larger tool. In addition, it is being requested that the wirebond pads be increased in size in the direction normal to the long edge of the board; this does not change the gap spacing between adjacent signals. Also, it should be noted that the V2.0 circuitry-side surface was entirely covered with solder mask except for pad openings. It is requested that this not be done for V2.1.

AlN Spacer – This piece is almost unchanged from the V1 design except its profile has been slightly adjusted in the wirebond and connector clearance areas.

Foot – The new design is significantly different from the V1 design. It is shorter and has scalloped sides to permit use with the new deep access manual wirebonder that has been ordered. Figure 2.1-1 shows the module from a 60° viewing angle and shows that the work area is visually accessible. This was demonstrated on one V2.0 module that was bonded on the deep access manual bonder at FCC, as mentioned above. It does not have separate raised sections for FPSP mating, relying instead on raised FPSP mounting regions for contact area control. Also, since the FPSP clearance hole for the CCDI/cable assembly must be widened to allow the cable & card to pass through the plate, the alignment pins and threaded mounting holes have been combined into pins with built-in threaded holes in order to save space. Additionally, threaded holes have been added for attachment of tooling to be used during module handling steps such as storage box loading or installation onto the FPSP. Previously, the fastening holes were also used for this task – this is certainly a possible way of doing this, but an unnecessary elegance. Four threaded handling holes have been added, as use of different hole positions may be desired depending on a modules position on the FPSP. For example, modules near an edge or near the VIB cards might be easier to install with the loading rods located as far as possible from any nearby obstructions. Finally, small protrusions in the connector clearance opening will be used to strain relief the connector to the foot (Figure 2.1-2). Connector solder joint

breakage was an issue for a few V1 modules, and this feature is being added here to prevent similar trouble. The protrusions occur at the level nearest the AIN, which reduces the length which distorts due to different thermal expansion behavior between the Invar, AIN, and AI.

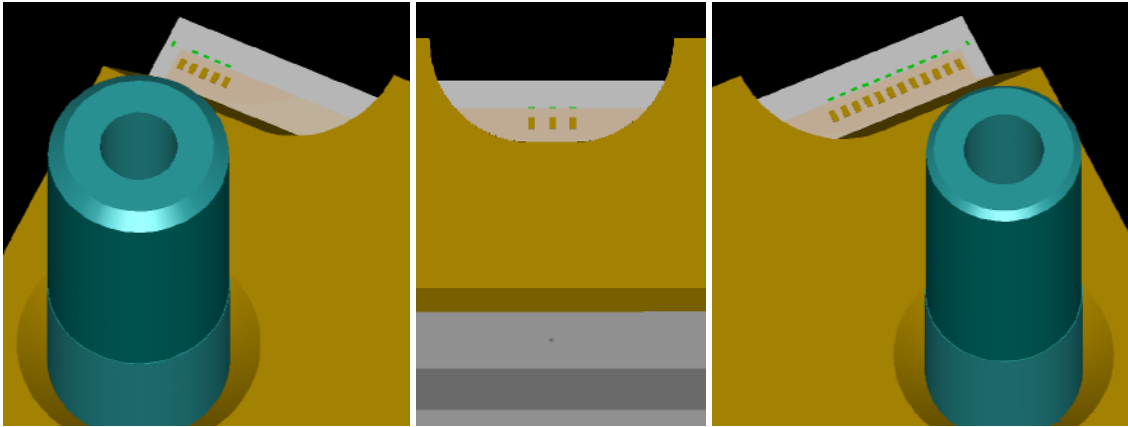


**Figure 2.1-1:** Images of Module Showing Viewability of Wirebonding Regions

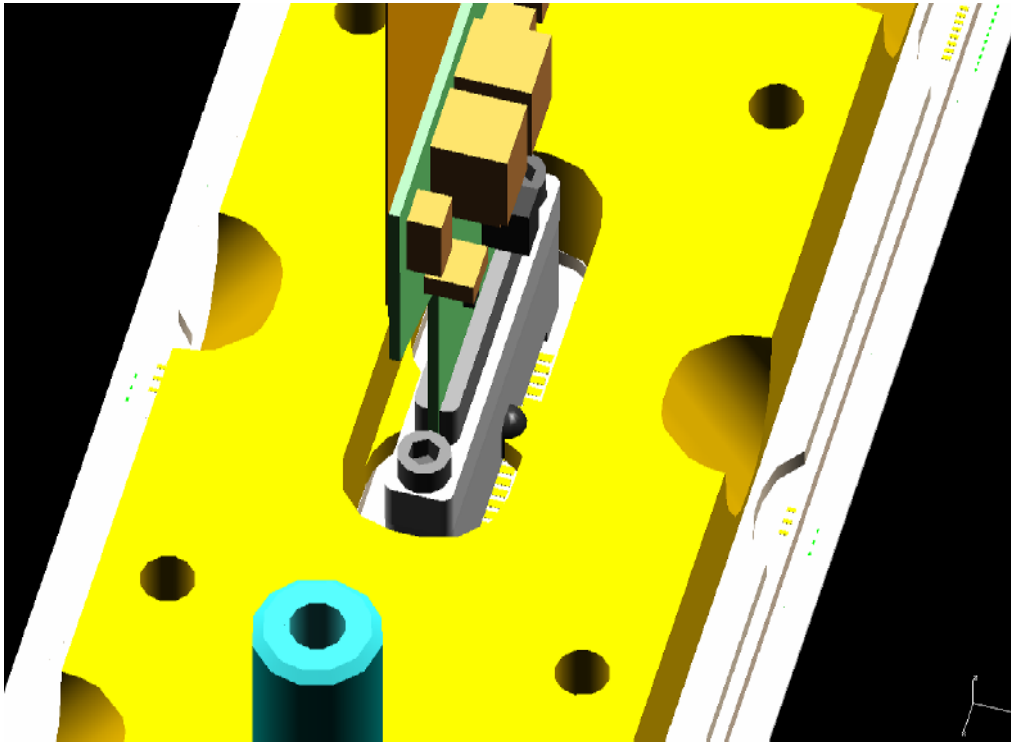


**Figure 2.1-2:** Images of Module Showing Connector Body Reinforcement

Mounting Pins – As discussed above, module fastening and locating features have been combined in to allow a larger FPSP cutout necessary since the CCDI card and cable are to pass all the way through the FPSP. Use of two different pin diameters prevents installation in the wrong orientation. The pins themselves are stepped in diameter, with several mm of pin nearest the foot providing a precise fit to the mating features on the FPSP, and the rest of the extending pin length at a slightly smaller diameter, which allows the long pin to provide accurate guidance during installation, thus minimizing the risk of contact with neighboring modules, while preventing the risk of the pins binding in the FPSP holes if they are not perfectly perpendicular to the foot's mounting face. An M3 threaded hole is located in the end of each pin.

Epoxy – All but one of the epoxy joints are to be made with the Epotek 301-2 epoxy used in V1, V2.0, and used for decades on CCDs by UCSC/Lick. As previously discussed [Refs 1,3], this epoxy has a very low viscosity and can be fed by capillary action into small gaps, where it is left to cure for 48 hours at room temperature. A thicker epoxy is needed to tack the sides of the Airborn connector to the connector restraint, so 3M Scotchweld 2216 will be used for this purpose. This adhesive was used on the later V1 and all V2.0 modules to reinforce the connector-to-AIN board joint and is commonly used for cryogenic and aerospace applications. Data sheets for these two epoxies can be found at the following sites:

<http://www.epotek.com/SSCDocs/datasheets/301-2.PDF>  
[http://multimedia.3m.com/mws/mediawebserver?66666UuZjcFSLXTtlx&X5x&\\_EVuQEcuZgVs6EVs6E666666--](http://multimedia.3m.com/mws/mediawebserver?66666UuZjcFSLXTtlx&X5x&_EVuQEcuZgVs6EVs6E666666--)

Weight Estimate – The weights for these components are estimated below. The sum of these weights is 94 grams.

CCD =	$(63.39 * 33.32 * 0.25) * 0.00233 = 1.2 \text{ g}$
Epoxy joint #1 =	$(61.72 * 29.97 * 0.13) * 0.00095 = 0.2 \text{ g}$
AIN readout board =	7.1 g (actual weight of V1 board with Airborn connector & RTD)
Epoxy joint #2 =	~0.2 g
AIN spacer =	$(1610 \text{ mm}^3) * 0.00326 = 5.2 \text{ g}$
Epoxy joint #3 =	~ 0.2 g
Foot =	$(9060 \text{ mm}^3) * 0.00805 = 72.9 \text{ g}$
5mm Pin =	$(348 \text{ mm}^3) * 0.00805 = 2.8 \text{ g}$
6 mm Pin =	$(516 \text{ mm}^3) * 0.00805 = 4.2 \text{ g}$

## **2.2 MODULE ASSEMBLY**

### **2.2.1 Outline of Assembly Steps**

The basic assembly outline is shown below. New tooling will have to be designed for many of these assembly steps, and this effort is scheduled to begin once the module design has been finalized. A detailed, step-by-step procedure will be written for each part of the assembly process, as was done for the previous pedestal and pictureframe modules (DES docdb #104). As has been done for previously-constructed units, paper travelers will be maintained for each CCD module to keep track of part serial numbers, technician name & date, special comments, etc.

1. Clean feet, pins, and AIN spacers as they are received
2. Inspect parts
3. Install pins into feet
4. Inspect installed pins
5. Construct AIN readout board subassy
  - a. Receive and clean AIN readout board
  - b. Install shorting plug into Airborn connector
  - c. Use jig to position spacer over readout board
  - d. Apply epoxy and allow to cure
6. Construct foot subassembly
  - a. Use jig to position foot onto AIN subassembly
  - b. Apply epoxy between foot and AIN spacer
  - c. Verify thickness of completed subassembly
  - d. Apply epoxy between foot and Airborn connector
7. CCD installation
  - a. Move CCD from Gelpak case to assembly jig
  - b. Position foot subassembly above CCD
  - c. Apply epoxy between CCD and AIN readout board
8. Module thickness inspection
  - a. Transfer CCD gluing jig top plate with module still attached to QC4000 CMM
  - b. Perform thickness inspection over a 15-point grid
  - c. Return to workbench
9. Wirebonding
  - a. Transfer CCD to wirebonding fixture
  - b. Package fixture in an ESD-safe container and take to the Lab D bonding room
  - c. Wirebond the 40 connections between the AIN board and the CCD using the new K&S 4523AD currently being purchased by FNAL
  - d. Repackage fixture in the ESD-safe container and return to Lab C south
10. Transfer module to storage box
11. Clean contamination from CCD surface as necessary
  - a. ESD-safe cleanroom swabs have been used with acetone to clean the CCD surface on pictureframe, V1, and V2.0 packages.
  - b. Use of a special formulation of "First Contact" cleaning polymer<sup>1</sup> doped with carbon nanotubes for ESD safety is currently being investigated.
12. Remove shorting plug from the Airborn connector and replace with the CCDI/cable assembly
13. Install module storage box into its storage container [storage box goes into test cubes during testing, storage container safety houses it in a static-dissipative, shielded enclosure for transport between work areas and long-term storage]
14. Deliver completed module for electrical and flatness testing

There are three major differences between this outline and the process used to fabricate the V1 and V2.0 modules. The first is that the CCD is not glued until later in the assembly sequence, which is now possible due to the planned use of the manual deep-access wirebonder. With bonding possible on a complete module, which required foot design changes, the CCD is not installed until the very last gluing step. This eliminates some CCD handling steps that were necessary when the CCD was installed prior to foot gluing, thus reducing ESD-related handling risks. Additionally, the different access clearances with the new bonder allow use of the real shorting plug during bonding rather than the temporary use of a conductive foam block inserted inside the connector. Removal of this block and

---

<sup>1</sup> See DES DocDB #664 and <http://www.photoniccleaning.com/>

replacement with the shorting plug is another ESD-risk step that is eliminated. It should be noted, however, that as a fallback the module design still allows use of the other automatic wirebonders at SiDet as long as bonding is done prior to foot gluing. However, doing so would impact the assembly fixture designs, requiring significant retooling, and this obviously precludes the benefits of deep access manual bonding described above.

The second major change from V1 and V2.0 is the elimination of the small tape pieces used to temporarily tack the CCD to the AlN readout board. Adapted from the UCSC/Lick design, and necessary for the original assembly techniques used, these small tape pieces (six pieces each about 1 mm square) are visible in the CCD images and have a noticeable impact on local CCD flatness. In order to eliminate them, a new assembly fixture must be developed that combines aspects of the V1 CCD gluing and foot gluing fixtures. The CCD must be held in a controlled location on a precision-flat surface (porous ceramic vacuum plate) while the foot / AlN subassembly is suspended above it at a precise height (to control overall module thickness) and accurate location (to control the relative position between the CCD and the foot's mounting pins). A small air gap will therefore be maintained between the CCD and the surface of the AlN readout board, and the Epotek 301-2 epoxy can then be fed into this gap by capillary action, as has been done previously. In this way, this step can be completed without the use of the tape squares. In addition, it should be noted that a few small bubbles have also been seen in the images from a few modules. This is believed to be a function of surface cleanliness and application technique, so care must be taken to ensure clean surfaces and a consistent application procedure.

The third major difference involves the installation of the CCDI/cable assembly as part of the module construction process. It is currently envisioned that this assembly is added at this time and that it is never removed, thus reducing handling of the connector, a few of which have been broken in the past. Although this does not directly change the assembly procedure, it does impact the module design (as discussed in Section 2.1). It also impacts module storage, which must now accommodate the card/cable, and module installation into the focal plane, which will have to control cable motion to prevent damage to neighboring modules on the FPSP.

### **2.2.2 Estimate of Production Workflow**

Using the task outline above, the flow for a full week's work and an effort estimate, based on experience with V1 and V2.0 fabrication, is tabulated in Table 2.2.2-1. "Assembly Chain 1" is geared towards producing the module foot subassembly (drawing 436409) at a rate of five per week. For the workflow shown, foot subassemblies are done in two separate chains, with these complete the day after Step 6D, which would be Mon & Tues. In order to split the work up so not all work is done on M/W/F, one of these chains had steps moved to T/Th (recall that the Epotek 301-2 epoxy takes 48 hours to cure). This helps level the workload, but increases the number of fixtures required since five or more foot subassemblies are undergoing the same step at the same time. Note also that the "Assembly Chain 1" work does not involve the CCD and therefore is not ESD-sensitive.

"Assembly Chain 2" is involved in gluing & wirebonding the CCD and completing the module. It again is split up into two sections, with groups of 2 or 3 modules being processed together. Wirebonding effort is listed separately from Tech time to emphasize that few Techs are trained to do this work.

In addition to the effort shown, extra effort is required for other tasks such as unpacking of newly-delivered CCDs from LBNL, fabrication of pictureframe modules using sample sensors from each foundry lot, etc. Also, time will be spent on part and supply inventory management, work area cleaning & control, equipment upkeep, etc., so Table 2.2.2-1 does not reflect the full effort needed.

It is recommended that at least two Techs be trained to do each task. This includes having the wirebond group manager trained to do this work as a backup. The mechanical tech group manager should also be trained to be familiar with this work so they can help provide oversight and serve as backup when needed. During production, it is therefore assumed that the following resource fractions will be needed:

- 2 Techs (includes both mech & wirebonding)
- 0.25 Sr. Tech. (includes both mech & wirebonding managers)
- 0.5 Engineer

**Table 2.2.2-1: Assembly Workflow Estimate**  
[Step #'s from workflow outline above]

Day	Assembly Chain 1A		Assembly Chain 1B		Assembly Chain 2A		Assembly Chain 2B		Total Effort (hours)
	Task	Effort (hr)	Task	Effort (hr)	Task	Effort (hr)	Task	Effort (hr)	
M	Step 5: AIN/AIN gluing [qty=3]	Tech = 3 ME = 1	Step 6C&D*: Ft. / connector gluing [qty=2]	Tech = 2 ME = 0	Step 7: CCD gluing [qty=3]	Tech = 4 ME = 1	Steps 10-14*: Module completion [qty=2]	Tech = 3 ME = 1	Tech = 12 ME = 3
T	---	---	Step 5: AIN/AIN gluing [qty=2]	Tech = 3 ME = 1	Day available for part prep, storage box assembly, etc. [Tech = 4, ME = 2]				Tech = 7 ME = 3
W	Step 6A&B: AIN/Foot gluing [qty=3]	Tech = 3 ME = 1	---	---	Step 8: Thk. Meas. [qty = 3]	Tech = 1 ME = 3	Step 7: CCD gluing [qty=2]	Tech = 4 ME = 1	Tech = 8 Bonding = 4 ME = 6
Th	---	---	Step 6A&B: AIN/Foot gluing [qty=2]	Tech = 3 ME = 1	Step 9: Wirebond [qty=3]	Bonding = 4 ME = 1	---	---	Tech = 6 ME = 3
F	Step 6C&D: Foot/ connector gluing [qty=3]	Tech = 2 ME = 0	---	---	---	---	Step 8: Thk. Meas. [qty = 2]	Tech = 1 ME = 2	Tech = 3 Bonding = 3 ME = 3
Sat / Sun	---	---	---	---	---	---	Step 9: Wirebond [qty=2]	Bonding = 3 ME = 1	---

\* - Process continued from previous week's work.

Summation of Effort<sup>2</sup>:    Tech:            36 (excludes bonding), with a maximum of 12 in one day  
    Bonding:        7, with a maximum of 4 in one day  
    ME:              18, with a maximum of 6 in one day

<sup>2</sup> Additional effort required beyond the tasks outlined in this table, as described in Section 2.2.2.

### 2.3 MODULE THERMAL ANALYSIS

The temperature gradient through the module was predicted<sup>3</sup> as shown below. The following conditions were assumed:

- Mounting face temperature = -100°C (so three-digit results display indicates tenths of a degree)
- Radiative heat flux on CCD =  $1 * \sigma * (293^4 - 173^4) = 367 \text{ W/m}^2$  heat flux or  $367 \text{ W/m}^2 * (0.0634 * 0.0333 \text{ m}^2) = 0.775 \text{ W / CCD}$
- CCD Amplifier = 40 mW maximum [Refs 1,2] (modeled as always on)
- RTD = 1.5 mW [DES docdb 329] (no impact, but added anyway as a continuous load)

The same material properties assumed in the FEA studies documented in Ref 2 were also used here.

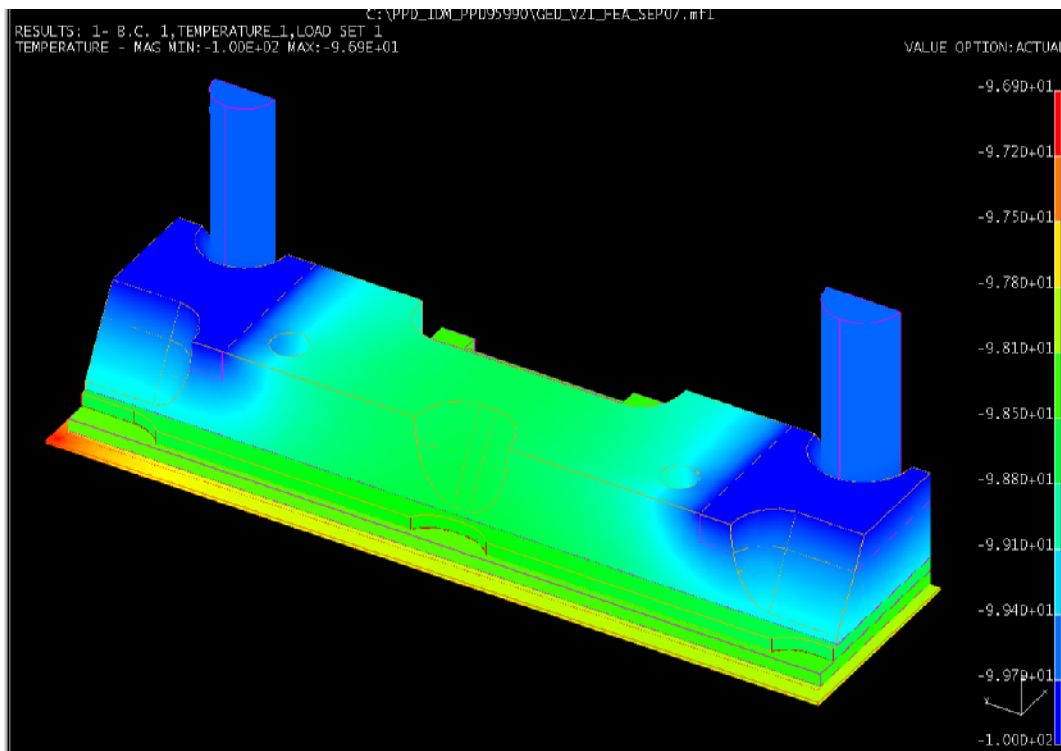


**Figure 2.3-1:** Temperature range within module ~3.1°C

The temperature at the RTD was predicted to be 98.2°C. Gradients within the AlN pieces are small, as the poorer-conducting epoxy tends to even out the ceramic temperature. The foot temperature gradient is ~1.4°C. The silicon temperature gradient is shown in Figure 2.3-2. The temperature in the active area is uniform to within 1°C, with the amplifier corner experiencing some gradient.

<sup>3</sup> Ideas case V21\_2X4\_MODULE-FEA

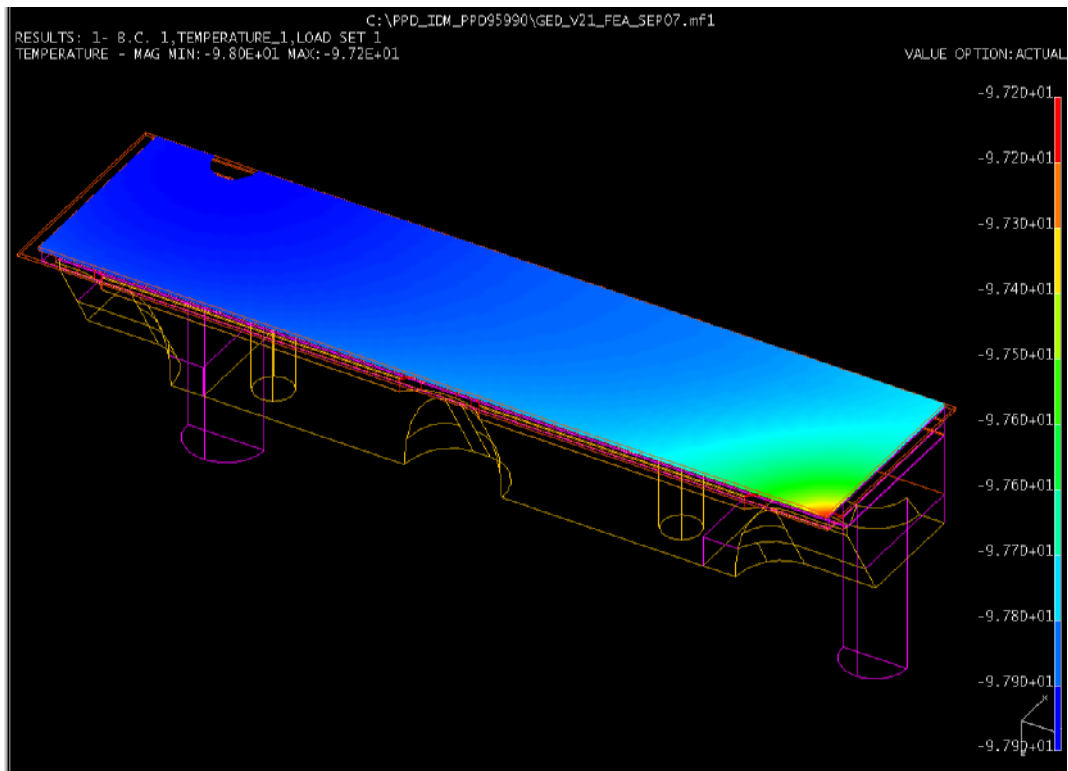


**Figure 2.3-2:** Temperature range within active silicon  $\sim 0.8^{\circ}\text{C}$

## **2.4 MODULE DEFORMATION AND STRESS ANALYSIS**

As discussed for previous studies, thermal deformation is expected due to differential thermal expansion between the various materials used. The material properties assumed for this study are documented in Ref 2. For this work, a  $\frac{1}{2}$ -module model was developed. Several studies to investigate various aspects of the design were done, and a thermal deformation summary of some of the lessons learned is included below:

- a. A 1-pound squeezing force applied along the length of the module (see Section 2.6.3 below) was found to have no effect on Si warpage.
- b. Pushing the AlN readout board out into the Si dead area in the area between bondfields had a negligible effect (and would complicate gluing, and possibly board fabrication).
- c. Changing AlN readout board and/or AlN spacer thickness by  $\frac{1}{2}$  mm had only a small effect.
- d. Making the AlN spacer the full width of the AlN board (except for bondfield region cutouts) was insignificant.
- e. Changing the foot thickness by 1 mm resulted in an insignificant difference.
- f. Gluing the connector to the protrusions on the foot slightly improves flatness by partially constraining the aluminum body material (compared to having the connector glued to the AlN only).

A particular difficulty in constructing this model was deciding how to simulate the connector. It was desired to have wings inside the foot's connector opening to reinforce the connector. This was requested since a few connectors were broken off their boards during connector mating/separation during early V1 work. The bottom of the connector body does not directly contact the AlN. Instead, the L-shaped 0.010" solder leads protrude down from the liquid-crystal polymer core (housed in the aluminum connector body) and the flats are soldered directly to the AlN board traces. The connector is then essentially perched on top of 37 very thin pins and therefore is not rigidly constrained to the board. However, since the connector will be rigidly attached to the foot, and the process could

conceivably be revised to rigidly attach it to the AlN board (by the addition of some epoxy there during construction, as was done during V1), the connector has been assumed here to be rigidly attached. This is modeled as an epoxy gap between the aluminum and the AlN. The 37 connector pins are not modeled.

Using the resulting module model, the thermal deformation was predicted<sup>4</sup> assuming the temperature profile generated in Section 2.2 above. The overall Z-direction (normal to the FPSP) deflection is shown in Figure 2.4-1. The negative values shown in the legend apply to the connector, which is shrinking upwards towards the AlN while the rest of the module is shrinking downwards towards its FPSP mounting face.

The deformation of the active area of the silicon is shown in Figure 2.4-2. It indicates a thermal distortion of 3.5 microns in this region. Roughly a micron of that is concentrated in the area of the connector. A separate model case with no connection between the aluminum and the AlN here indicated a distortion of 2.4 microns, as shown in Figure 2.4-3.

For the base case (with rigidly-attached connector), the stresses predicted in each layer are shown in the Figures 2.4-4 through 2.4-11. The maximum stresses for the V2.1 design are listed in Table 2.4-1 and are compared to the V1 FEA results.

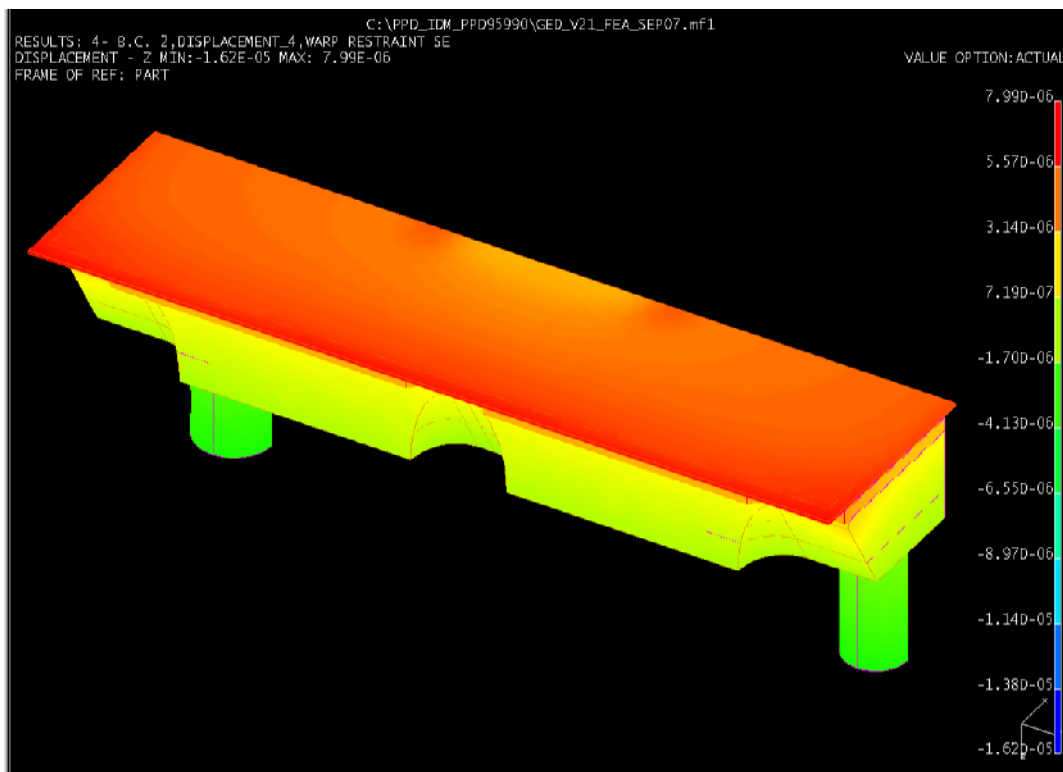
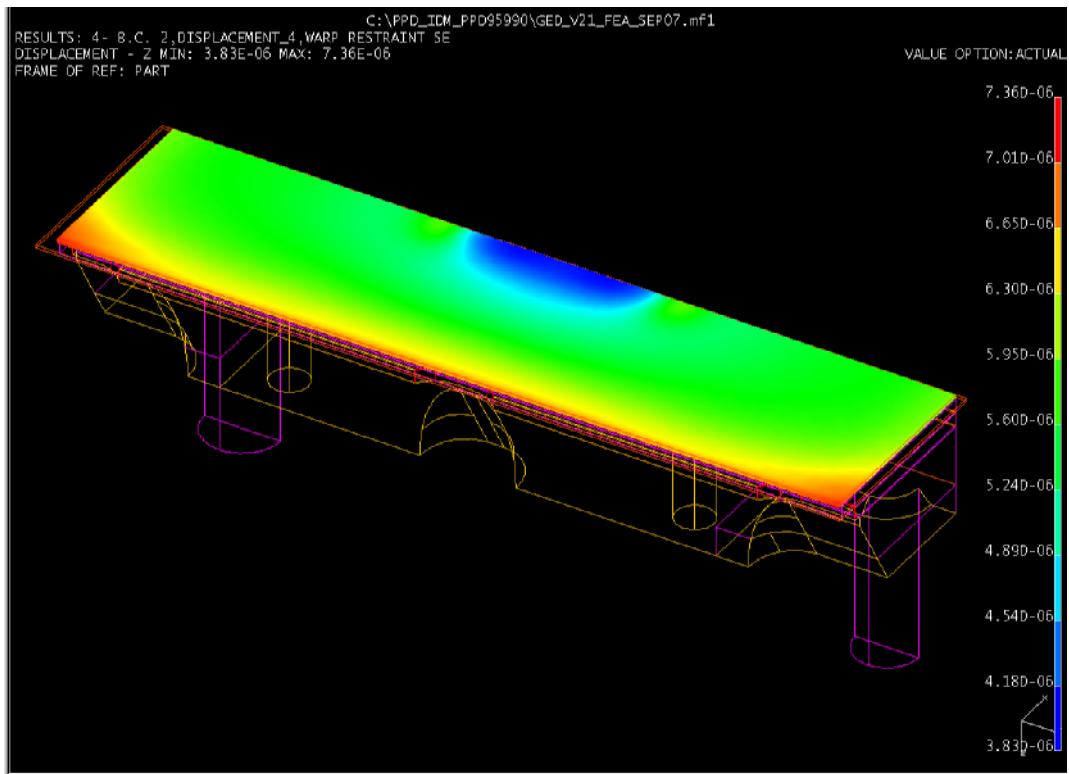
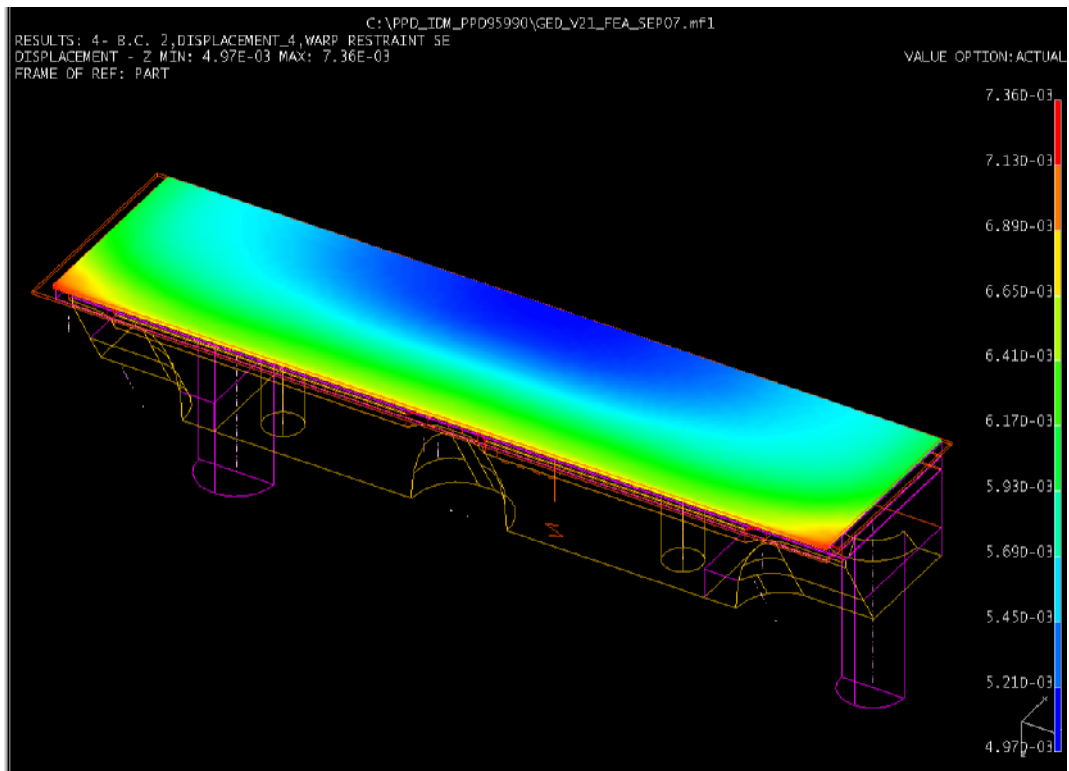


Figure 2.4-1: Thermal deformation of the module (m)

<sup>4</sup> Ideas case V21\_2X4\_MODULE-FEA



**Figure 2.4-2:** Thermal deformation of the active silicon area (m)  
 Peak to valley = 3.5 microns



**Figure 2.4-3:** Thermal deformation of the active silicon area  
 assuming no contact between the connector and the AIN readout board (mm).  
 Peak to valley = 2.4 microns

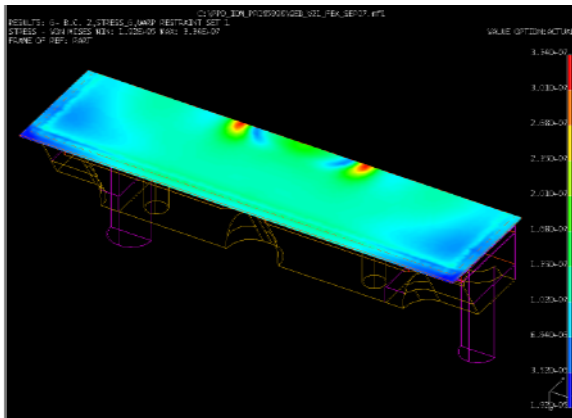


Figure 2.4-4: Stress in the Si (Pa)

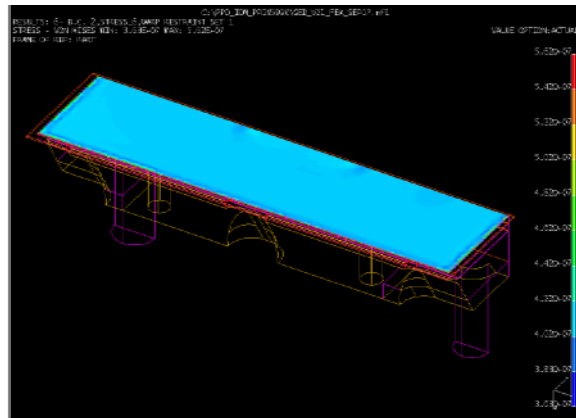


Figure 2.4-5: Stress in the Si/AlN epoxy (Pa)

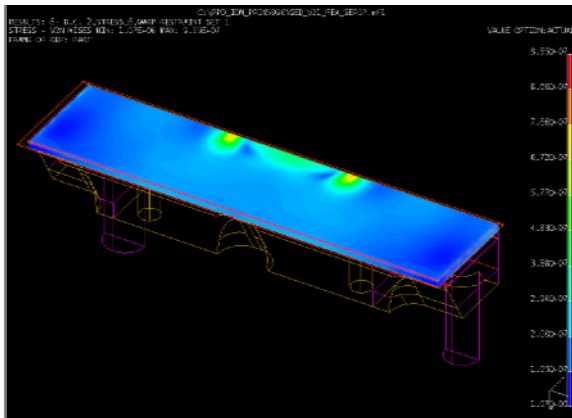


Figure 2.4-6: Stress in the AlN readout board (Pa)

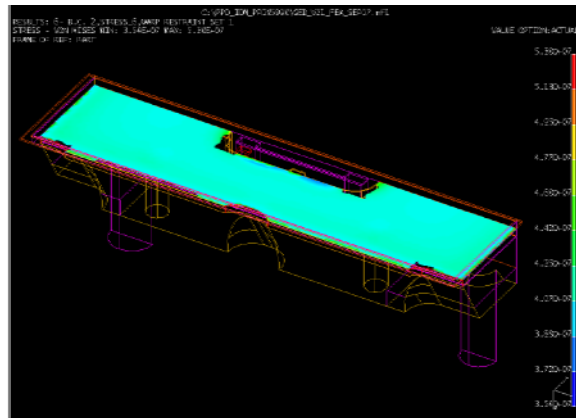


Figure 2.4-7: Stress in the AlN/AlN epoxy (Pa)

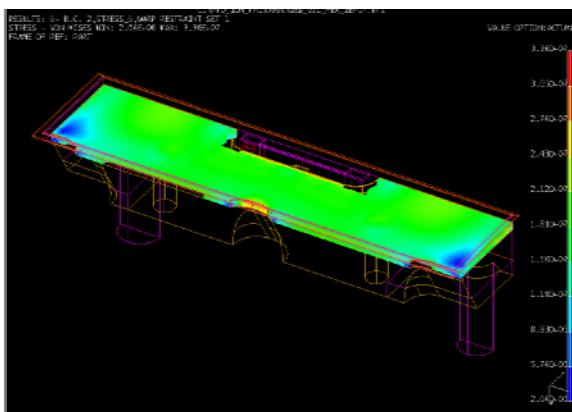


Figure 2.4-8: Stress in the AlN spacer (Pa)

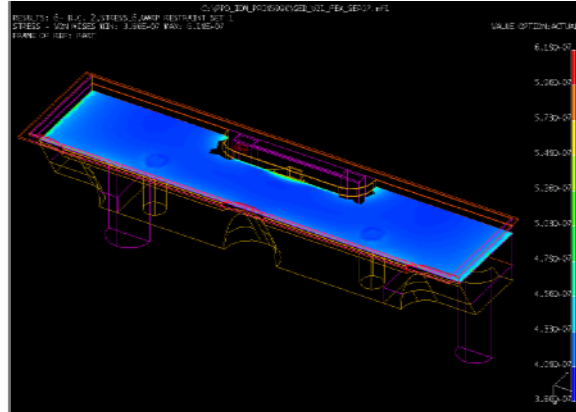


Figure 2.4-9: Stress in the AlN/Invar epoxy (Pa)

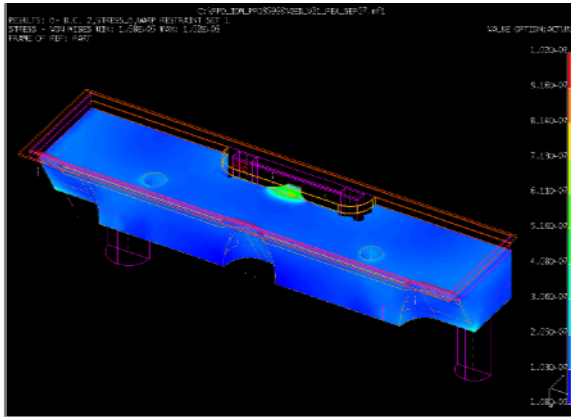


Figure 2.4-10: Stress in the foot (Pa)



Figure 2.4-11: Stress in the connector/foot epoxy (Pa)

Table 2.4-1: Estimated Module Stresses

Layer	Predicted V2.1 Stress (MPa)	Predicted V1 Stress [2] (MPa)	Stress Limit [2] (MPa)	Comments
CCD	33	14.9	120	Higher V2.1 stresses due to connector modeling, which was not included in V1.
Si-to-AIN Epoxy Layer	~ 44 (bulk)	~ 41 (bulk) max in module	~ 67	
AIN Readout Board	96	30 max in module	2100 comp. 280 tens.	Higher V2.1 stresses due to connector modeling, which was not included in V1.
AIN-to-AIN Epoxy Layer	~ 43 (bulk)	~ 41 (bulk) max in module	~ 67	
AIN Spacer	34	30 max in module	2100 comp. 280 tens.	
AIN-to-Foot Epoxy Layer	~ 43 (bulk)	~ 41 (bulk) max in module	~ 67	
Foot	~ 70	35	483	Max in connector reinforcement protrusions, which were not present in V1.
Foot-to-Connector Epoxy	~ 50	---		Edge effects higher.

## 2.5 MODULE FLATNESS CONSIDERATIONS

The flatness specifications for the CCDs are as follows:

- T28 RMS variations within 1 cm<sup>2</sup> are < 3 microns [Refs 2,3,9]
- T29 Adjacent 1 cm<sup>2</sup> regions are within 10 microns of each other [Refs 2,3,9]
- \* The focal plane shall be within an envelope of 30 microns peak-to-valley [the proposed Ref 9 conflicts with the older spec of 50 microns from Refs 2 & 3]

Thermal distortion, as considered in Section 2.4 above, is only one portion of the overall flatness. The following elements contribute to the total flatness:

### A. Module Thickness

Some module-to-module variation in an array is expected due to small differences in constructed thicknesses. Assembly tooling will be developed attempting to minimize this effect. Modules measured during the V1 effort (Ref 4) were found to be an average of 4.4 microns less than nominal with  $\sigma = 1.3$  microns, and similar results are expected for V2.1.

### B. Module Flatness at Room Temperature

The fabrication techniques attempt to construct as flat a module as possible, but some small variation over the surface of a CCD can still be expected. For the modules constructed for the V1 effort, Ref 4 documents the measured room temperature surface measurements and found an average peak-to-valley of 6 microns with  $\sigma = 2$  microns.

### C. Module Thermal Distortion When Cooled

As discussed in Section 2.4 above, FEA studies of the module indicate that thermal distortion on cooldown should be less than 4 microns.

It should be noted that for the V1 effort, flatness scans on cold CCDs (Ref 4), which measured the combined effects of elements "B" and "C" here, found that each of the seven devices measured satisfied the "T29" requirement. Only five out of the seven passed "T28", but the failures were thought to be related to use of the small tape squares between the CCD and the AIN. This tape is being eliminated for the V2.1 design.

### D. FPSP Flatness at Room Temp

The flatness of the mounting surfaces on the FPSP depends on the machining limits. For the V1 focal plane mockup, this was tolerated as an envelope of 5 microns [per drawing ME-436131]. The V2 FPSP should be fabricated with very tight flatness requirements.

### E. Focal Plane Distortion When Cooled

As the system is cooled, some small thermal distortion is expected. Section 2.6.3 below discusses the module/FPSP frictional force effect. But a more detailed consideration of this effect, and other potential FPSP cooldown influences, is not within the scope of this study.

### F. Focal Plane Distortion with Telescope Orientation

The focal plane is expected to distort by some small amount as the camera is rotated about the sky, but this effect is not within the scope of this study.

## **2.6 MODULE INTERFACE WITH THE FOCAL PLANE SUPPORT PLATE (FPSP)**

A section of the FPSP is shown in Figure 2.6-1 below and in the drawing on the following page. Overall thickness was maintained consistent with the V1 plate design, but the thickness should be validated as part of the upcoming FPSP design & analysis effort. Instead, this modular representation has been developed here and is documented in drawing 436407 as an input to that design task.

The FPSP has raised precision-flat regions for CCD foot mating. Pin engagement with the modules includes one hole and one slot to allow for variations in machining tolerances and for differences in thermal contraction rates between the aluminum plate and the Invar feet. The module is to be held in place with spring-loaded shoulder screws that are bottomed out on the faces of the module's alignment pins. These mating points protrude 1 mm from the bottom of the clearance pocket in which the screws sits. Since the screw shank diameter is larger than the pin's mating holes in the FPSP, this sets a limit beyond which the module cannot be moved before further motion is prevented. Additional access holes are provided for CCDI/cable clearance and for loading rod access. There are no trapped air volumes in this design (except for the connector internals).

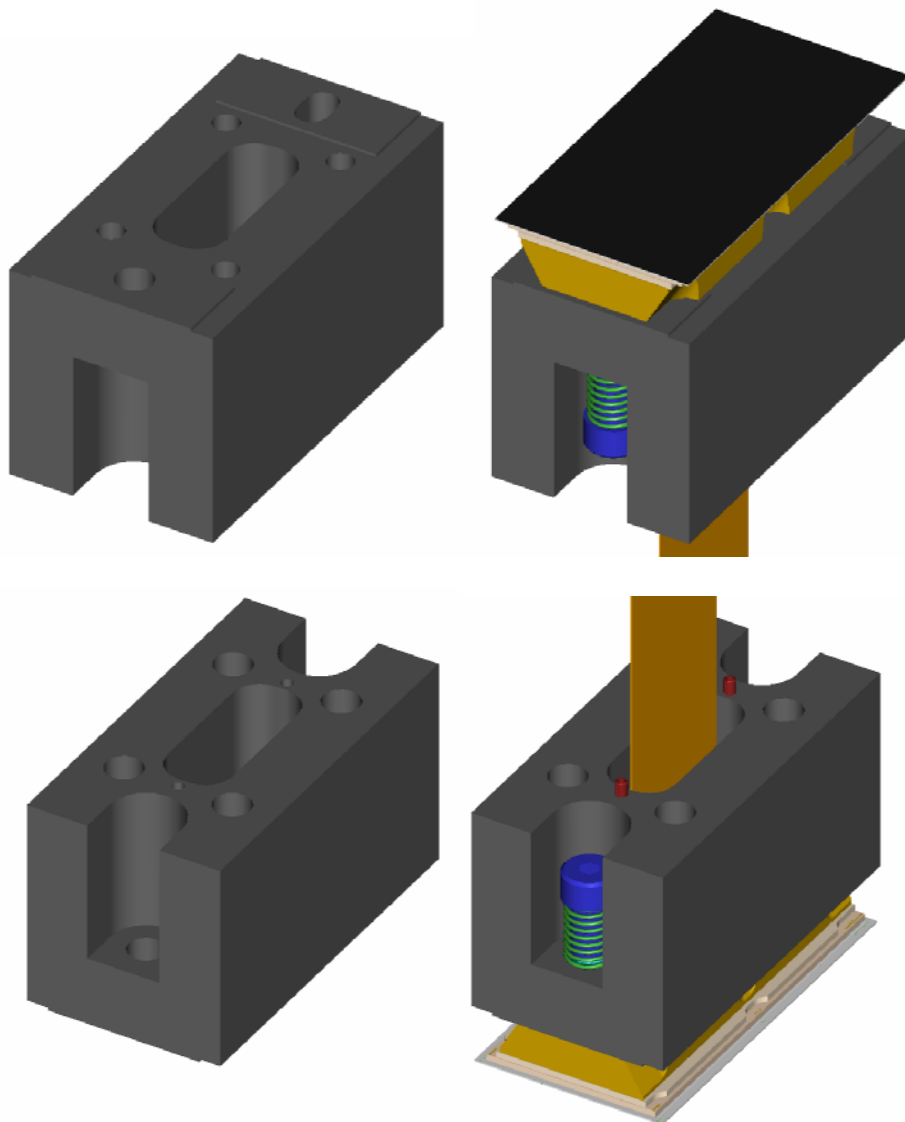
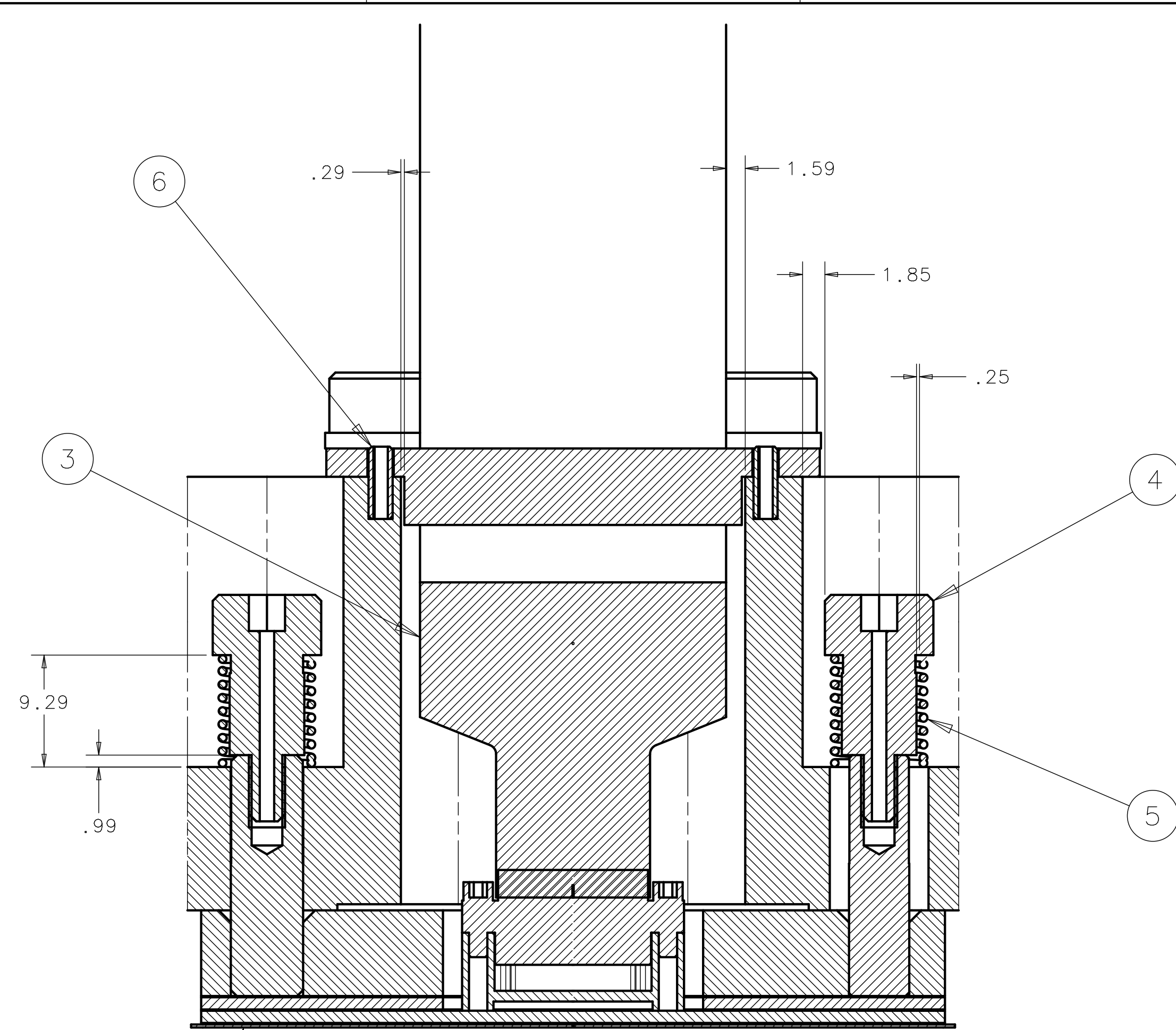
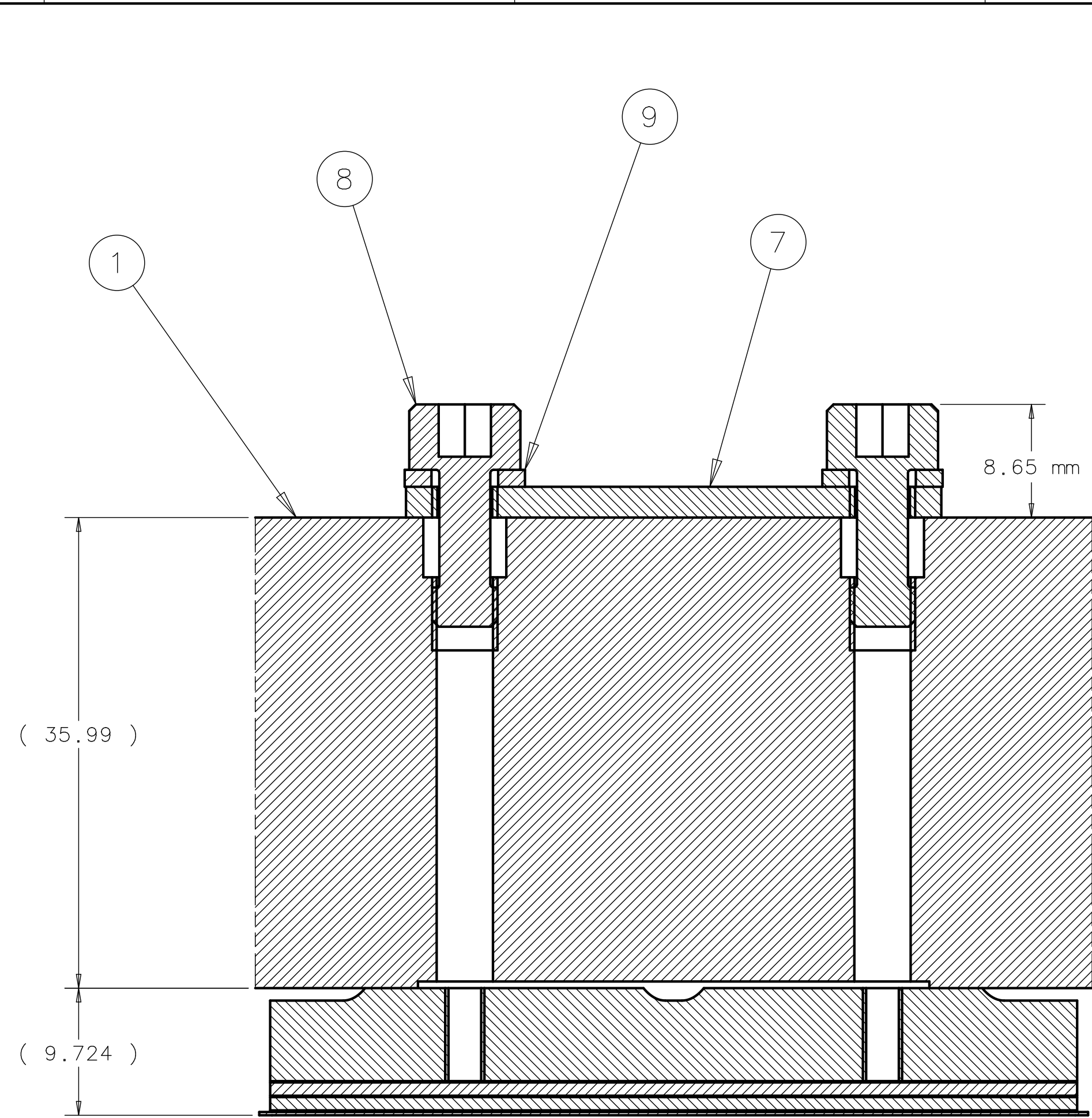


**Figure 2.6-1:** Section of FPSP Behind One CCD Module

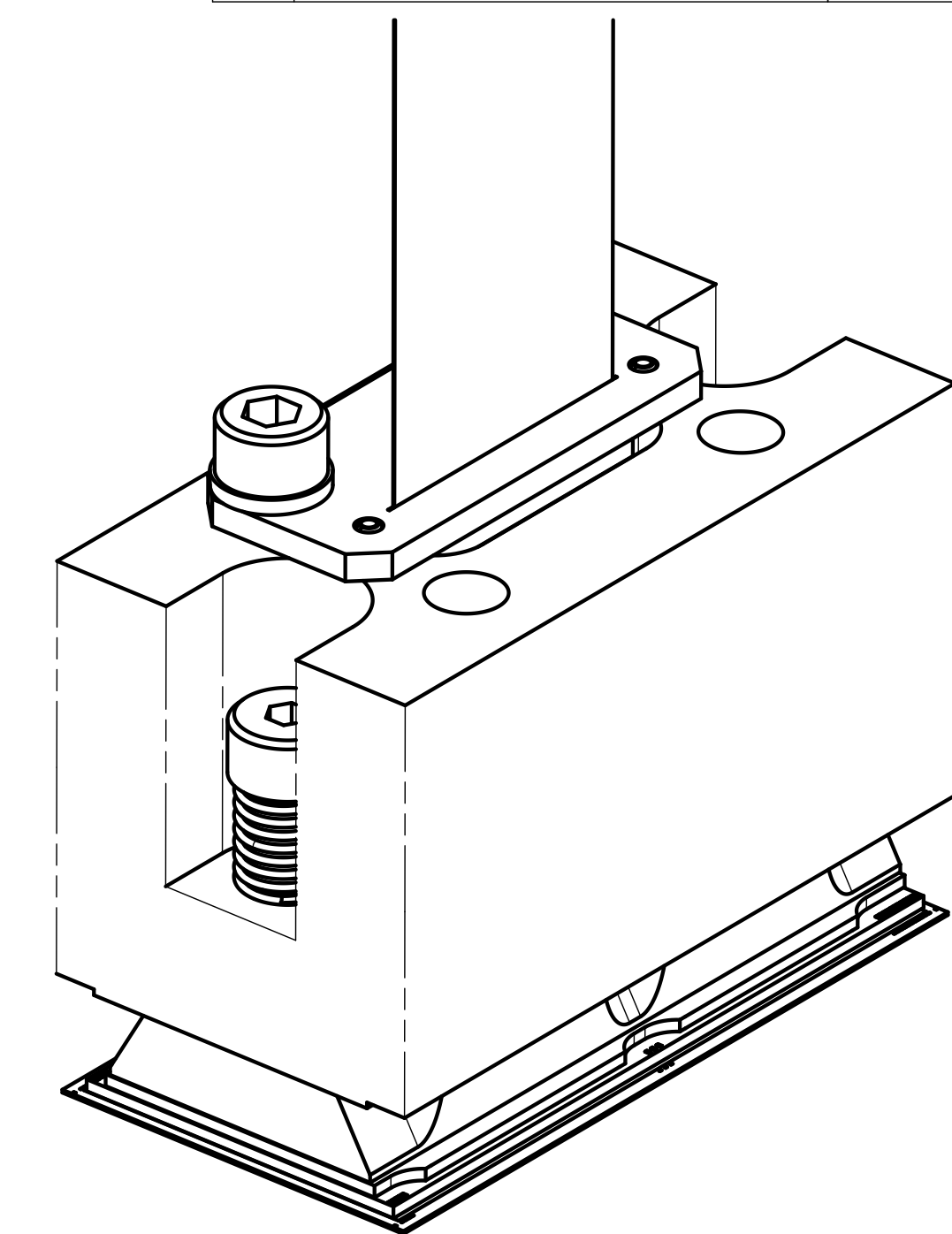
Not shown here is a cable constraint concept that is positioned on the red pins shown and bolts to threads that extend a partial distance inside the loading rod mounting holes. This restraint concept is still very preliminary and requires additional development effort, but is shown conceptually in Section 2.6.4 below.



SECTION A-A

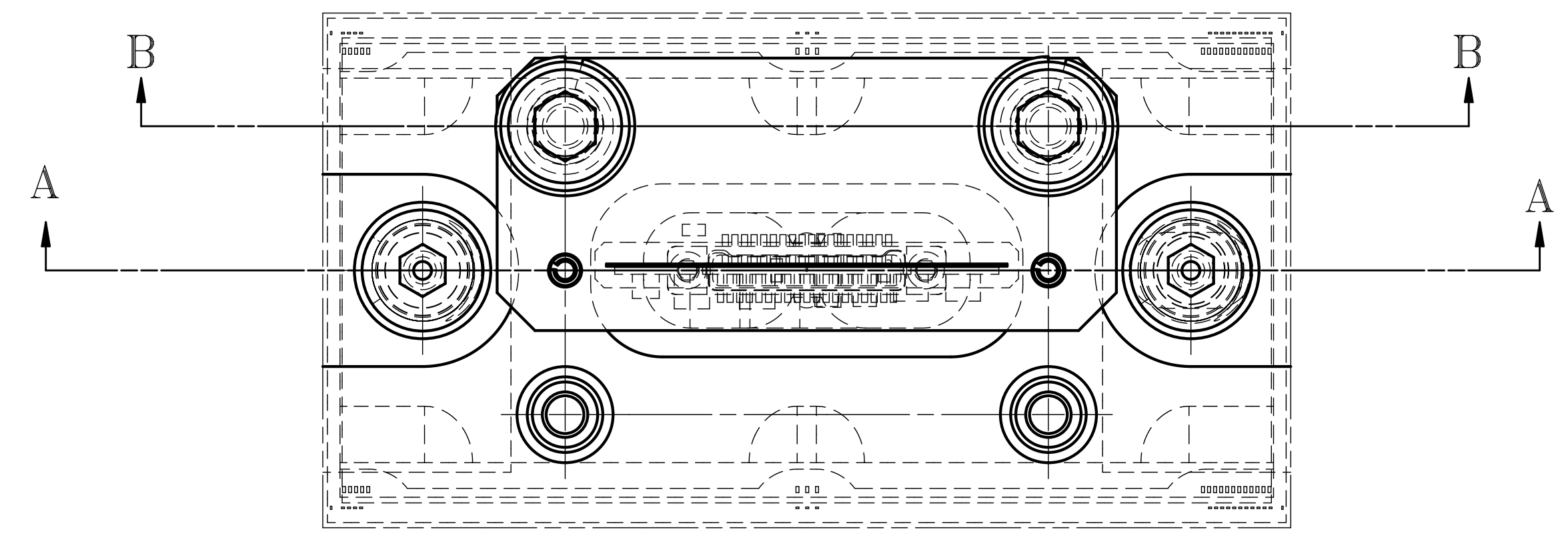


SECTION B-B



ISOMETRIC VIEW

SCALE =2:1



ITEM	PART NO.	DESCRIPTION OR SIZE	QTY.
9	MISUMI P/N SSLW5	SPRING WASHER, 5MM	2
8	MISUMI P/N GUTB5-3-12	PANEL MOUNT SCREWS, 5MM	2
7	MB-436417	CABLE RESTRAINT PLATE	1
6	MISUMI P/N SSPSR2-6	SPRING PIN, 2MM	2
5	MISUMI P/N UF8-15	MOUNTING SPRING	2
4	MB-436416	V2.1 MOUNTING SCREW	2
3	MB-436415	V2.1 CCDI CABLE ASSEMBLY	1
2	MC-436408	V2.1 2K X 4K CCD ASSEMBLY	1
1	MC-436407	FOCAL PLANE SUPPORT PLATE SAMPLE SECTION	1

PARTS LIST

UNLESS OTHERWISE SPECIFIED	ORIGINATOR	G. DERYLO	12-SEP-2007
.XX	.XXX	ANGLES	DRAWN
± XX	± XXX	± X	CHECKED
1. BREAK ALL SHARP EDGES X MAX.		APPROVED	H. T. DIEHL
2. DO NOT SCALE DRAWING.		USED ON	---
3. DIMENSIONS BASED UPON ASME Y14.5M-1994		MATERIAL	SEE PARTS LIST ABOVE
4. MAX. ALL MACH. SURFACES 125			
5. DRAWING UNITS: U.S. INCH			

**FERMI NATIONAL ACCELERATOR LABORATORY**  
UNITED STATES DEPARTMENT OF ENERGY

**CTIO BLANCO DECAM**  
V2.1 2K X 4K CCD MODULE  
MODULE / FPSP INTERFACE LAYOUT

NOTICE: IMAGE OBTAINED FROM FERMILAB WEB SITE  
This information is provided for REFERENCE use only.  
Not for MANUFACTURE, or DESIGN INFORMATION.  
All information contained in this document represents work sponsored by an agency of the U.S. Government. Neither the U.S. Government nor any agency thereof, nor Universities Research Association, Inc., nor any of their employees or officers, makes any warranty, express or implied, or assumes any legal liability or responsibility for the accuracy, completeness, or usefulness of any information, apparatus, product or process disclosed, or represents that its use would not infringe privately owned rights.

SCALE 3:1 AS NOTED	DRAWING NUMBER 4900.122-MD-436406	SHEET 1 OF 1	REV
CREATED WITH : Ideas12NXSeries		GROUP: ACCELERATOR MECH. SUPPT.	

Detailed aspects of the interface are discussed below, including pin fits, module-to-module gap management, and determination of the appropriate mounting spring force.

### 2.6.1 Module Mounting Pin Fit

Fit of the mounting pins must be considered for both room temperature and cold conditions for both the press fit and slip fit engagements. Pins pressed into the focal plane were also considered, but the improved engagement lengths possible with the pins pressed into the feet led the design in that direction. The slip and press fits at +20 and -100°C are shown in the spreadsheet below for 5 and 6 mm pins. 5 micron pin diameter tolerances are assumed. Hole tolerances of 5 microns in the Invar and 12 microns in the FPSP are assumed. The room temperature values in this table are used to define sizes for the foot, FPSP, and mounting pin drawings.

1.DL/L Material Values					Mark's Fits	
					Inches	MM
Aluminum:	0.99745				RC2	0.0015
304 Stn. Stl:	0.99823				RC2	0.0065
Invar:	0.99980				FN2	-0.0020
					FN2	-0.0100
<b>Invar Pin Set 1</b>						
		Room Temp.	-100 C		R.T. Inches	
FP Support Plate (Aluminum)	Max	5.031	5.018		0.1981	
	Min	5.019	5.006		0.1976	
Pin (Invar)	Max	5.000	4.999		0.1969	
	Min	4.995	4.994		0.1967	
Module Foot (Invar)	Max	4.988	4.987		0.1964	
	Min	4.983	4.982		0.1962	
Pin / FP Plate Fit (slip)	Max	0.036	0.024		0.0014	
	Min	0.019	0.007		0.0007	
Pin / Foot Fit (press)	Max	-0.017	-0.017		-0.0007	
	Min	-0.007	-0.007		-0.0003	
<b>Invar Pin Set 2</b>						
		Room Temp.	-100 C		R.T. Inches	
FP Support Plate (Aluminum)	Max	6.033	6.018		0.2375	
	Min	6.021	6.006		0.2371	
Pin (Invar)	Max	6.000	5.999		0.2362	
	Min	5.995	5.994		0.2360	
Module Foot (Invar)	Max	5.988	5.987		0.2357	
	Min	5.983	5.982		0.2356	
Pin / FP Plate Fit (slip)	Max	0.038	0.024		0.0015	
	Min	0.021	0.007		0.0008	
Pin / Foot Fit (press)	Max	-0.017	-0.017		-0.0007	
	Min	-0.007	-0.007		-0.0003	

A CMM inspection performed on a set of four V2.0 feet found that the pins were perpendicular to the foot to an average of 1.36 mrad (~14 microns over 1 cm) with a maximum of 2.97 mrad (~30 microns over 1 cm). This concern leads to three actions:

1. The pins will be slightly stepped such that only a few mm of engagement will be the precise fit shown in the table above. The remaining pin length will be slightly narrower in order to still provide reliable guiding during installation but will be loose enough to prevent binding due to small tilts.
2. Greater care should be taken to guide the pin during foot assembly – the simple jig used has too much slop.
3. The assembled feet should be surveyed on the CMM prior to module construction to verify that pin insertion is reliable.

## **2.6.2 Module-to-Module Gaps**

The CCD layout provides a nominal gap between sensor edges of 0.5 mm at room temperature. Several factors must be controlled in order to prevent edge-to-edge contact.

- a. CCD edges must be controlled relative to the module's mounting pins.
- b. The pin fits between the module and the FPSP must be tight enough to control location but loose enough to allow installation and prevent binding.
- c. The FPSP's locating features must be positioned accurately.
- d. During installation, the mounting pins must not allow excessive tilting that might result in contact.
- e. When cooled, FPSP shrinkage must not allow the gap to close.

Item A: Silicon edge location relative to the foot's mounting pin was measured on several V1 modules, as documented in Ref 4. It was found that the average edge deviation was 0.030 mm, with a maximum measured deviation of 0.038 mm. It is expected that the V2.1 modules will be built with similar accuracy, but an allowance of 0.050 mm will be assumed.

Item B: Diametral pin slip fits are listed above in Section 2.6.1. As an added conservatism, this misalignment study will assume the FPSP hole is 25 microns larger than allowable:

5 mm Pin:	Room Temp	= 0.5 * (5.031 + 0.025 – 4.995) = 0.031 mm
	-100°C	= 0.5 * (5.018 + 0.025 – 4.994) = 0.025 mm
6 mm Pin:	Room Temp	= 0.5 * (6.033 + 0.025 – 5.995) = 0.032 mm
	-100°C	= 0.5 * (6.018 + 0.025 – 5.994) = 0.025 mm

Item C: The mounting feature positions for the FPSP are assumed to be true position toleranced to 0.002 in (0.050 mm) or better. This effect can be magnified by a factor of  $(0.5 * 63.39 / 25.4 = 1.25)$  since a portion of the module sticks out past the mounting pins. As an added conservatism, this misalignment study will assume that this is exceeded by 50%, for a maximum radial deviation of  $(0.050/2) * 1.25 * 1.5 = 0.047$  mm.

Item D: The pin/hole/slot clearance allows some tilting during installation, which translates to some lateral motion. The resulting offset can be found by looking at the amount of possible tilt with the pin against the edge of the top of the hole, as calculated below. This is only a concern during installation (warm, not cold). A layout drawing showing maximum tilting for oversized FPSP holes and minimized pin diameters is attached below and predicts a maximum tilt of 0.131 mm.

Item E: The aluminum focal plate will shrink more than the modules when cooled to -100°C, effectively reducing the gap between modules. The cold gap is found as follows:

$$\begin{aligned} \text{Gap along short edge} &= [(1 - 0.00255) * 63.890] - [63.382 \text{ cold Si length}] = 0.345 \text{ mm} \\ \text{Gap along long edge} &= [(1 - 0.00255) * 33.816] - [33.312 \text{ cold Si length}] = 0.418 \text{ mm} \end{aligned}$$

Summations: The different components are added up below:

$$\begin{aligned} \text{Warm} &= A + C + D < 0.250 \text{ mm} \\ &= (0.050) + (0.047) + (0.131) \\ &= 0.228 \text{ mm} \end{aligned}$$

This value represents 91% of the allowable 0.250 mm and is therefore just acceptable. Of course, adjacent modules are not installed simultaneously, so this is conservative.

$$\begin{aligned} \text{Cold} &= A + B + C < E / 2 \\ &= (0.050) + (0.025) + (0.047) \\ &= 0.122 \text{ mm} \end{aligned}$$

This value represents 71% of the allowable  $0.345/2 = 0.173$  mm and is therefore acceptable.

4

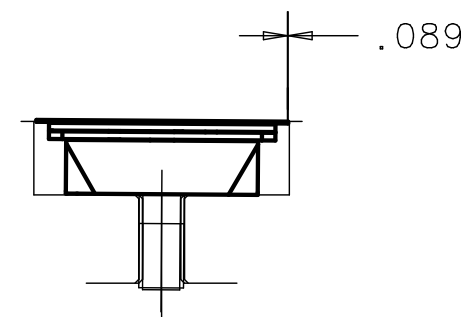
3

2

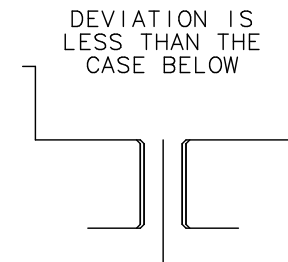
1

REV	DESCRIPTION	DRAWN	DATE
		APPROVED	DATE

5 MM

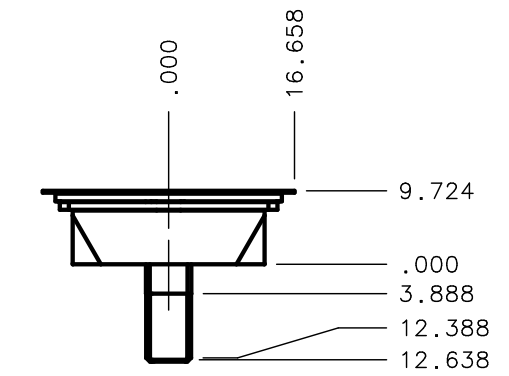


FPSP Contact / Max Hole Dia

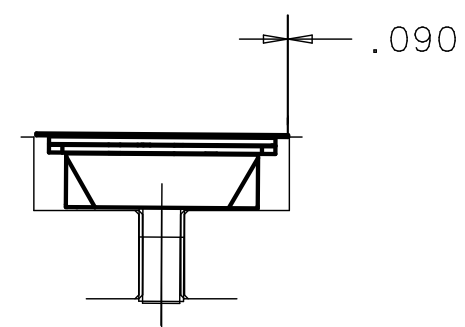
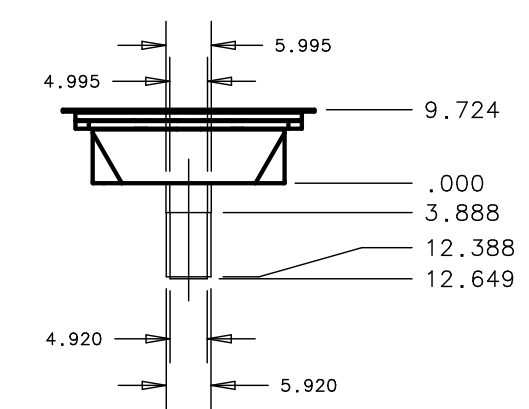


FPSP Contact / Max Hole Dia + 0.025mm

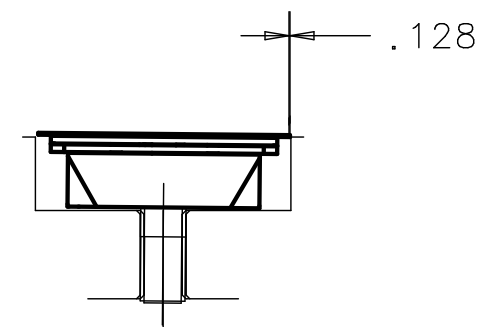
MODEL :



SYMBOL :

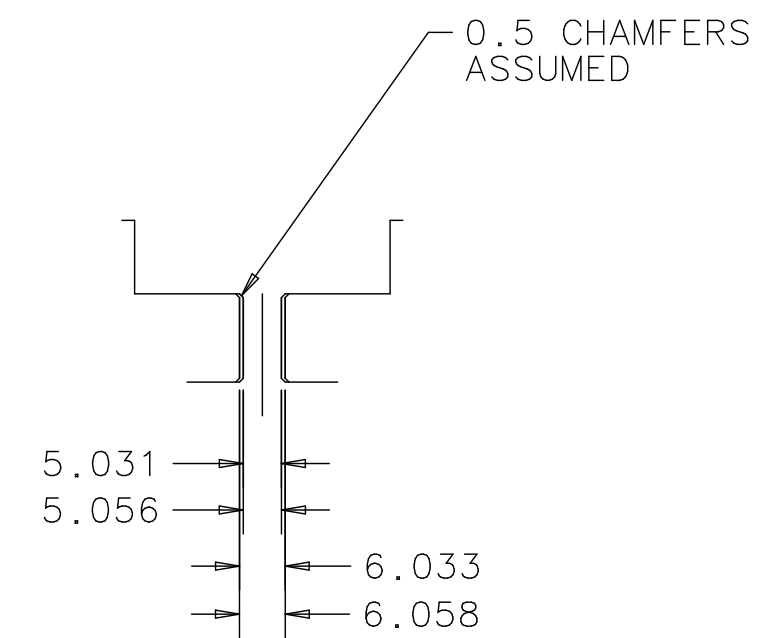


Elevated Position / Max Hole Dia

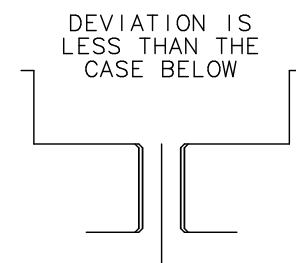


Elevated Position / Max Hole Dia + 0.025mm

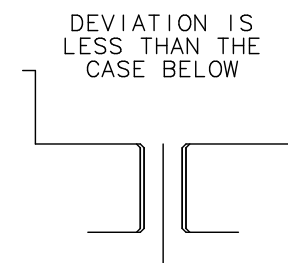
FPSP :



6 MM



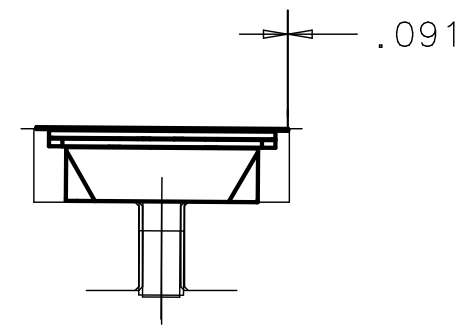
FPSP Contact / Max Hole Dia



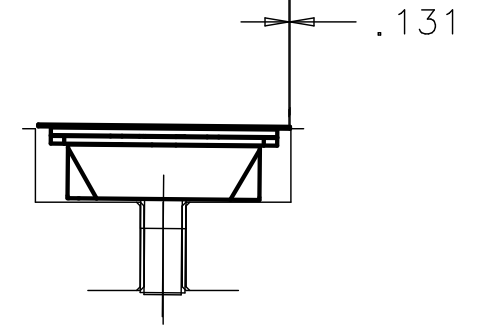
FPSP Contact / Max Hole Dia + 0.025mm

UNLESS OTHERWISE SPECIFIED			ORIGINATOR	
			DRAWN	
±	±	±	CHECKED	
1. BREAK ALL SHARP EDGES MAX.			APPROVED	
2. DO NOT SCALE DRAWING.			USED ON	
3. DIMENSIONS BASED UPON			MATERIAL	
4. MAX. ALL MACH. SURFACES				
5. DRAWING UNITS: ✓				

 **FERMI NATIONAL ACCELERATOR LABORATORY**  
**UNITED STATES DEPARTMENT OF ENERGY**



Elevated Position / Max Hole Dia



Elevated Position / Max Hole Dia + 0.025mm

SCALE	DRAWING NUMBER	SHEET	REV
		1 OF 1	
CREATED WITH :		GROUP :	

4

3

2

1

### 2.6.3 Module Mounting Spring Force

The mounting springs must provide enough force to keep the CCD seated against the FPSP but must provide a small enough force to allow relative sliding motion between the foot and the FPSP due to differences in thermal contraction behavior between the aluminum plate and the Invar feet. As a demonstration of why this is required, an FEA of a simplified version of the V1 focal plate was performed to study the effect of rigidly clamping the modules to the support plate. The CTE difference between the Invar modules and the aluminum plate causes an estimated 1020 microns of warpage at -100°C, as shown in Figure 2.6.3-1. In order to minimize this effect, the modules must therefore be allowed to slip relative to the plate so these interaction forces don't build up and cause such deformation.

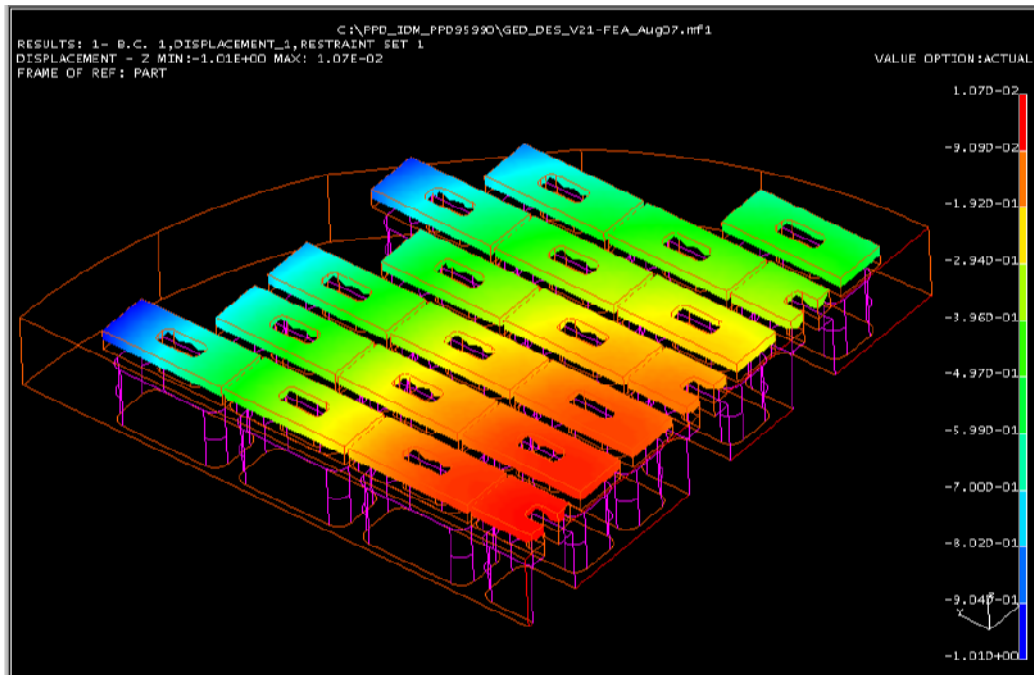


**Figure 2.6.3-1:** Thermally-induced 'Z' deformation of the focal plane for CCD modules rigidly attached to the V1 support plate. Other effects (e.g.; gravity) are not included.

In order to gauge the sensitivity of the support plate flatness to the amount of frictional force applied by the modules, another FEA<sup>5</sup> was run on a simplified V2-type plate assuming a stretching force of 1 pound per module was applied (force applied on opposing faces of the connector clearance hole). This stretching of the upper surface results in a Z warpage of 5.3 microns, as shown in Figure 2.6.3-2. In order to limit this effect to less than 3 microns, the maximum friction force is 0.57 pounds (linearity assumed over this range) before sliding between the feet and the plate relieves built up stresses. Assuming a friction coefficient of 0.61<sup>6</sup>, the maximum normal load between the module and one of the contact pads on the FPSP is  $0.57 / 0.61 = 0.93$  pounds (421 grams-force).

<sup>5</sup> Ideas case *FEA-FPSP\_TEST\_1LBF\_SPREAD*

<sup>6</sup> Steel to aluminum value from <http://www.engineershandbook.com/Tables/frictioncoefficients.htm>

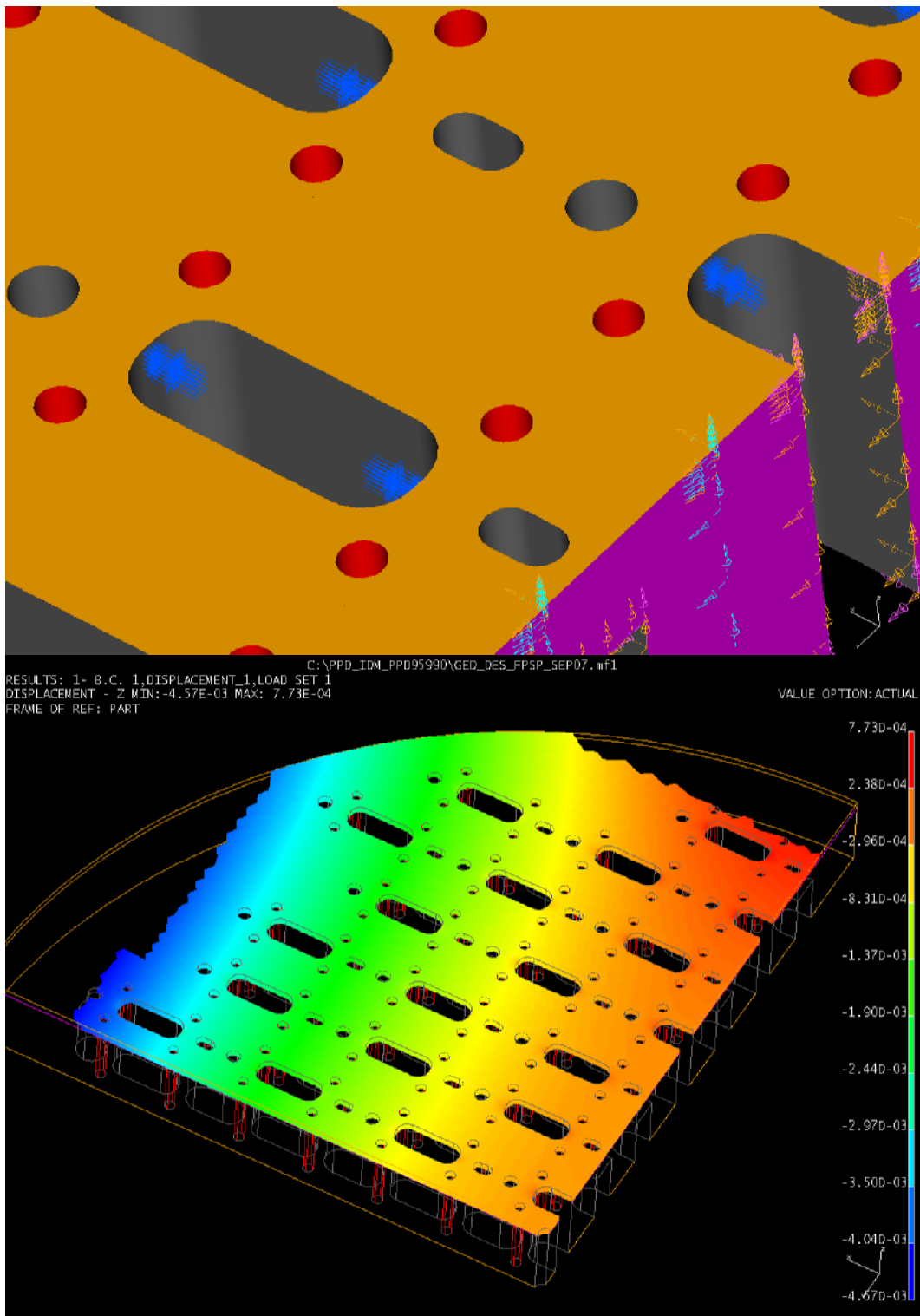


**Figure 2.6.3-2:** Focal plane support plate ‘Z’ distortion for a 1 pound spreading force per module applied on opposing faces of the connector opening

When the telescope is pointed at zenith, the total amount of spring force will be reduced by the sprung weight of the module (module, CCDI, and fastening hardware). Although the telescope is not pointed down as far as the horizon, this is the orientation in which the maximum normal force will be considered. Assuming use of Misumi USA spring # UF 8-15 (304 stainless steel), which has a spring rate of 0.049 kgf/mm and a free length of 15 mm, this leads to the following spring force determination:

- Maximum spring force at -100°C = 0.42 kgf
- The amount of spring force is reduced by 30% to conservatively account for uncertainty in the friction coefficient and the small effect from variations in the fabrication tolerances of the spring, screw length, pin length, FPSP thickness, etc. The nominal spring force is therefore 0.29 kgf.
- Spring force at room temp after adjusting by difference in spring material elastic modulus (difference in spring and other hardware dimensions is insignificant) =  $0.29 \text{ kgf} * (\sim 95\%) = 0.28 \text{ kgf}$
- For a 0.049 kgf/mm spring rate, a 0.28 kgf load requires a 5.70 mm deflection
- The hardware design should therefore compress the springs to  $15 - 5.7 = 9.3 \text{ mm}$
- Drawing 436406 shows a nominal compressed height of 9.29 mm
- This 5.7 mm of compression is less than the allowable  $0.45 * 15 = 6.75 \text{ mm}$  for this spring

When pointed above the horizon, the actual spring force is reduced due to the gravitational load on the spring weight. This effect is greatest at zenith. Sprung weight is estimated as follows:

- Module 94 g (from Section 2.1 above)
- Mounting screws  $2 * (557 \text{ mm}^3) * 0.0080 = 8.9 \text{ g}$
- Mounting springs  $2 * (0.5 * 0.6 \text{ g}) = 0.6 \text{ g}$  (direct measurement)
- CCDI card assy  $\sim 10 \text{ g}$
- Therefore, total sprung mass  $\sim 114 \text{ g}$
- At zenith, the clamping force is reduced to  $2 * 0.29 - 0.114 = 0.466 \text{ kgf}$
- Total spring force (cold) / sprung weight: Zenith =  $0.466 / 0.114 = 4.1$   
Horizontal =  $(2 * 0.29) / 0.114 = 5.1$

The springs can therefore resist a shock load of 4.1 to 5.1 G's in the camera's axial direction (depending on orientation) before the clamping force is reduced to zero and the module can momentarily lift off the FPSP. Per Ref 10, shocks of different levels are expected during earthquakes, general handling, and shipping. The largest shocks predicted are for truck loads, which are 3.5-g longitudinal, 2-g lateral, and 6-g vertical. It is recommended that camera shipping be planned to keep shocks to less than that required to lift the modules.

A sufficiently large shock in the transverse direction could overcome static friction between the feet and the FPSP and allow small shifts in module positions. Assuming a clamping force of 0.466 kgf at zenith and a static friction coefficient of 0.61, a force of 0.284 kgf is needed to initiate motion. Dividing by the sprung weight, this results in a shock resistance of 2.5 g's. Operation on the telescope is not expected to exceed this value, and earthquake loading is only 0.65 g's [Ref 10].

## **2.6.4 MODULE INSTALLATION**

The process outlined here is presented as an initial concept for further consideration. The figures below provide a basic description of the process. As a final plan is developed, detailed written procedures will be documented for use during this work.

The sequence in which CCDs must be installed on the FPSP is not covered here, but it should be noted that this is a topic that must be considered in detail, as must field replacement of a module during camera maintenance at CTIO. The camera model/mockup currently being fabricated in Lab B should be useful tool for investigating this issue.

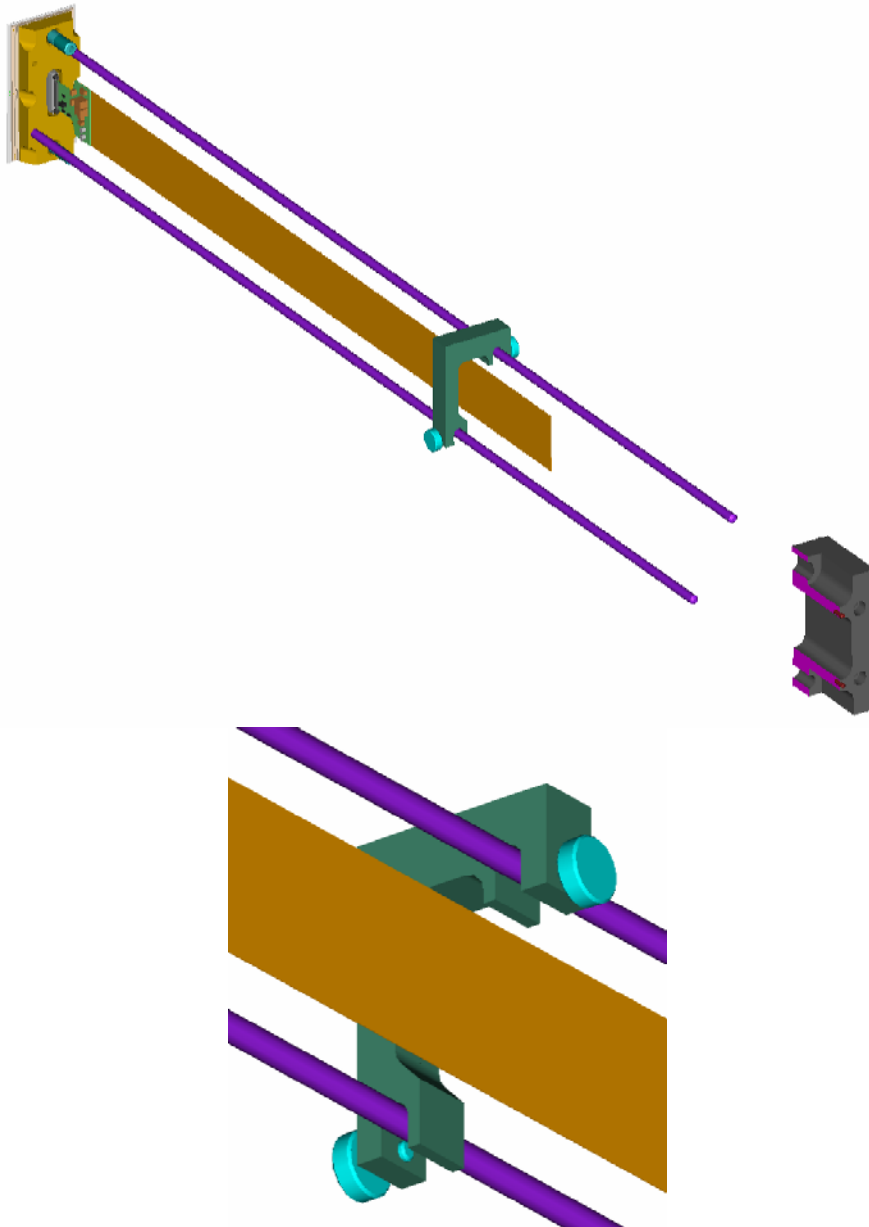


**Figure 2.6.4-1:** Initial approach, with close-up of installation rod bracket

The figure above shows the initial setup's approach to the array. The FPSP section behind a single CCD module is shown in the lower right and has been cut in half for a clearer view of its internals. Loading rods are first inserted into two of the four holes in the Invar foot while the module is in its storage box; the rods are then used to lift the module out of its box and are used as handles as one approaches the camera from the front (window) side. The installation rod bracket shown in dark green is a concept intended to temporarily tie the two rods together for

improved rigidity and therefore firmer handling of the module & rods as a single unit. The guide rods fit into slots in the bracket and are captured with thumb screws for ease of engagement/disengagement. Different bracket configurations would be needed when using a different set of foot holes. Here, opposite corner holes are used, as these provide the longest lever arm. For modules in the positions along the VIB, two holes along a long edge, furthest from the VIB, will likely have to be used due to limited accessibility here. The great length of these rods is necessary due to the presence of the readout cable, as the rod lengths should allow them to pass through the FPSP and partially out the rear before the cable can reach the previously-installed CCDs.

The rods are carefully inserted into their holes in the FPSP until they stick out the back by some amount, as shown in Figure 2.6.4-2. A partner, working from the rear side of the camera, can provide this feedback. Note that the rods can be fed into the FPSP holes more easily if one rod is slightly shorter than the other.

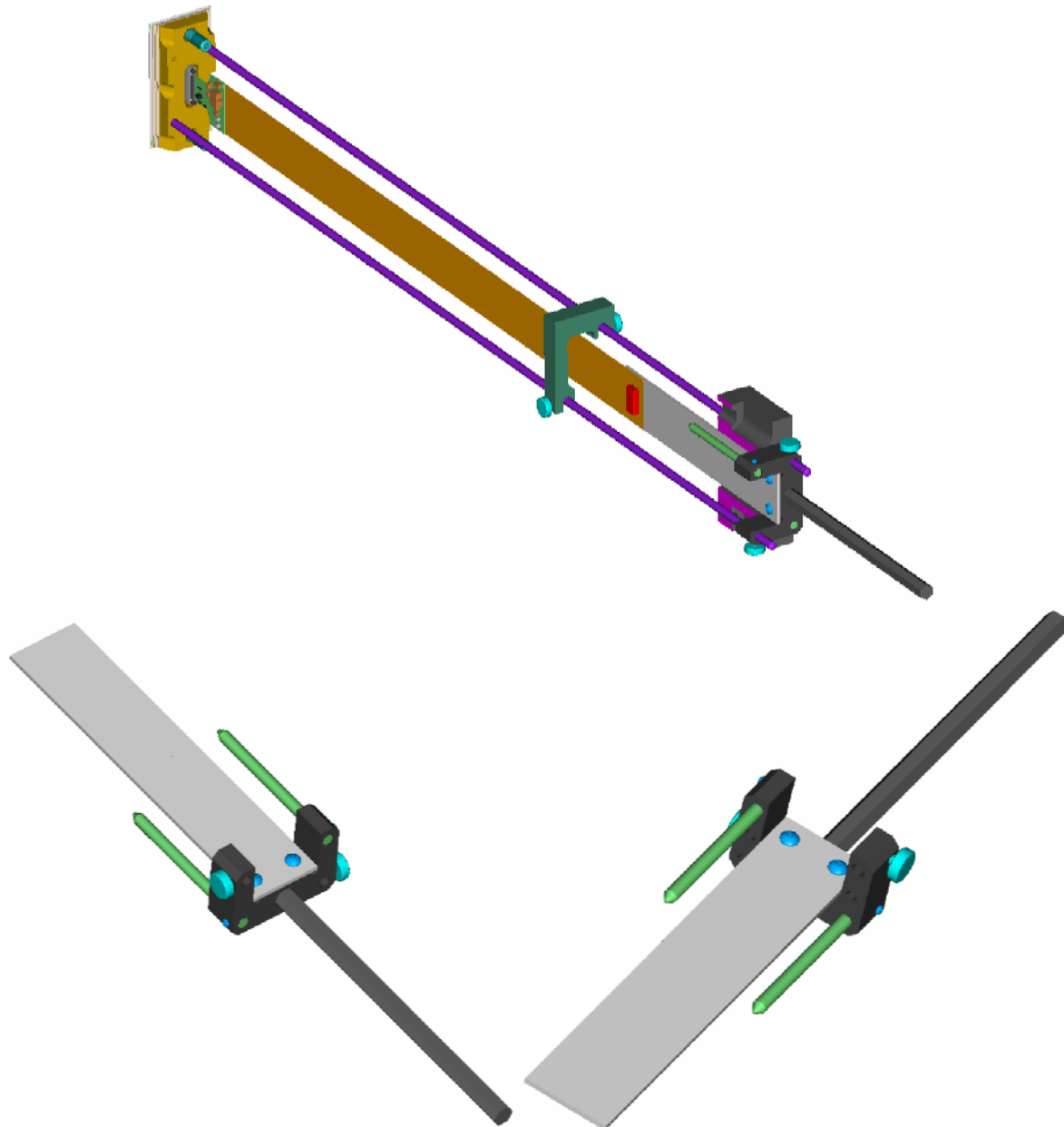
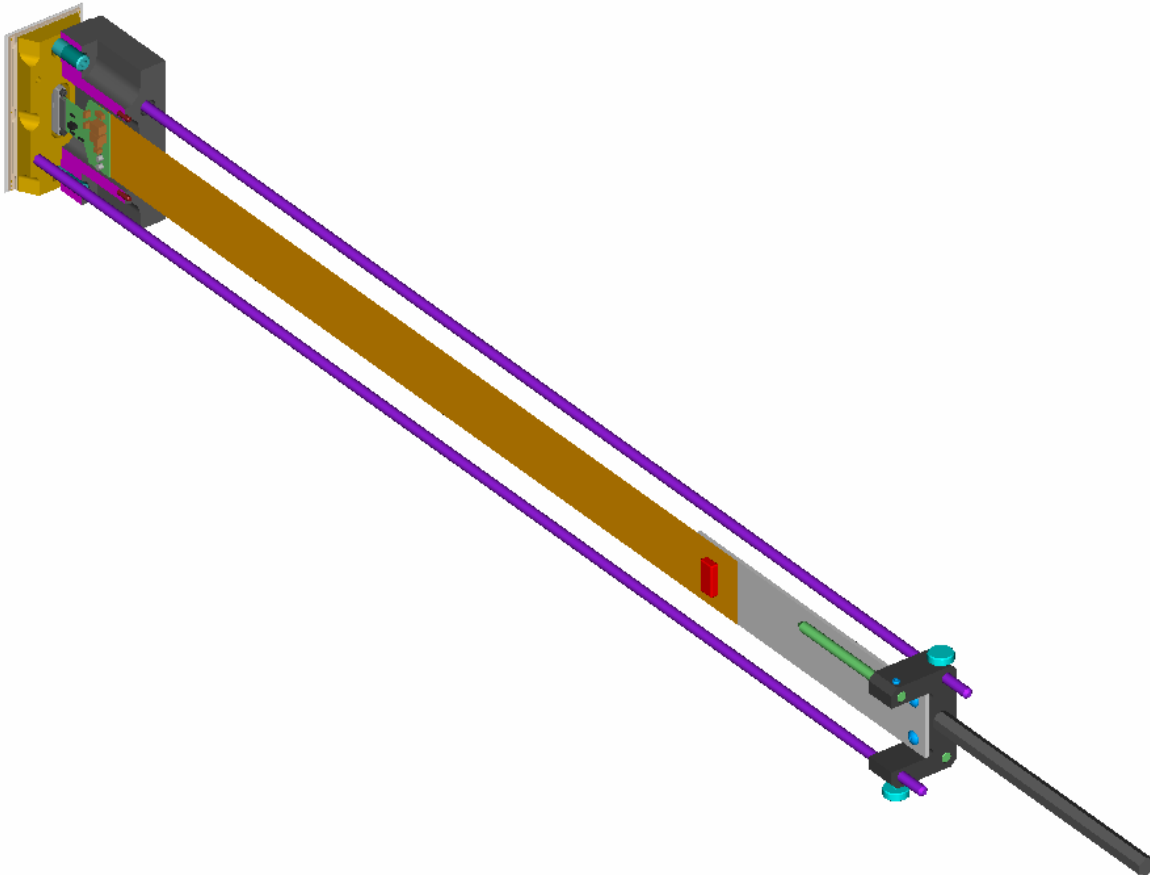


**Figure 2.6.4-2:** Installation tool concept, with close-ups

The figure above shows the engagement of an installation tool concept with the loading rods. This tool is installed from the rear and has a set of long pins that are inserted into the two unused loading rod holes for firm guidance and

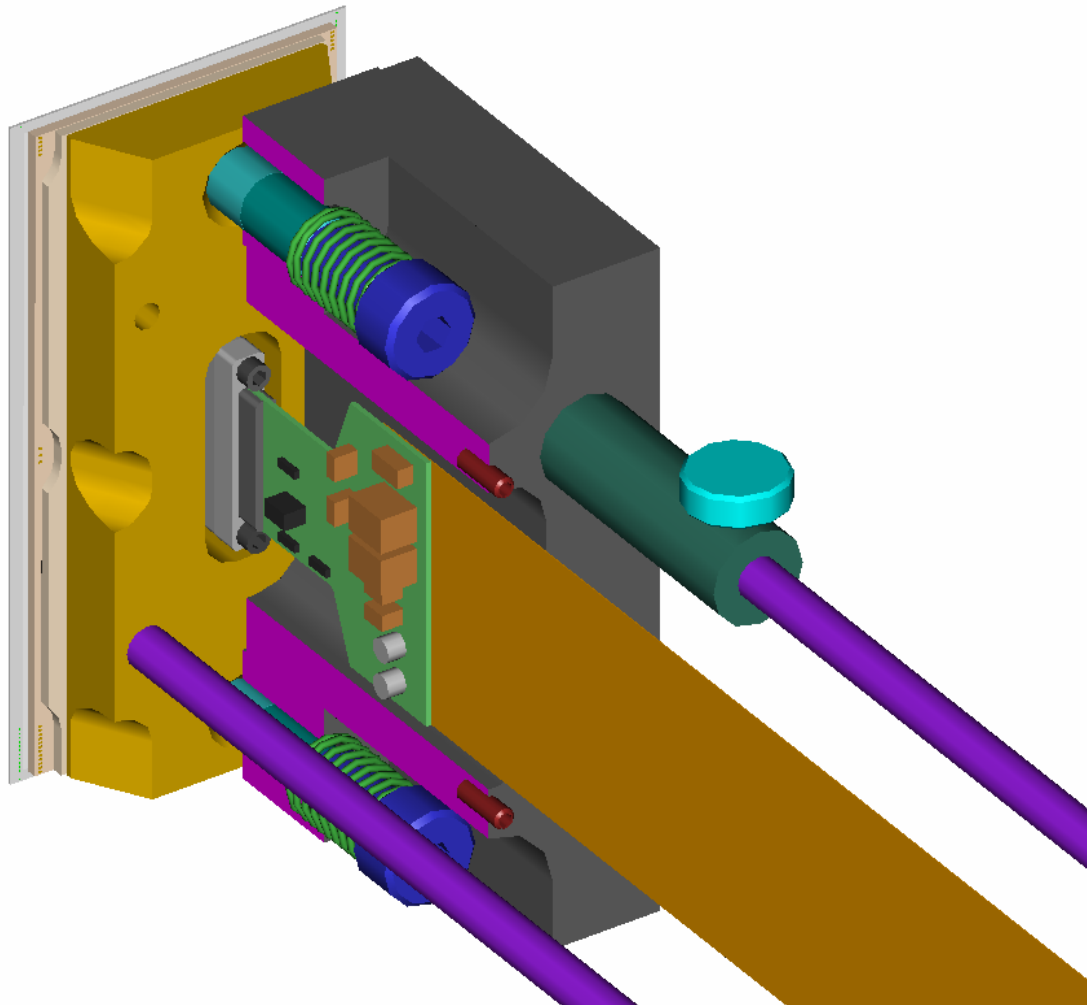
also has holes for the rods themselves, each with a threaded hole for a small thumb screw that is used to lock the rods to the tool. A steel diving board protrudes forward, through the FPSP's CCDI card & cable clearance hole, such that it overlaps with the end of the CCDI cable. A bar magnet can then be used to hold the cable in place against the diving board. This manipulation should occur safely forward of the rest of the CCD array. The dark green installation bracket can also be removed at this time, as it is no longer needed once the rods are engaged in the FPSP (and the bracket cannot pass through the FPSP anyway). A handle protrudes from the back of the installation tool for handling convenience. Note that a modified version of this tool may be needed, with the two upright sections of the U-shaped tool removed, for use near the VIB.

Figure 2.6.4-3 shows the installation tool drawn back by the person behind the vessel until the module is seated in place on the FPSP, with the person in front of the vessel providing feedback. Experience with the V1 modules in the multi-CCD test vessel found that gap control was an issue due to poorly machined plate holes and relatively short module pins. The alignment pins (and loading rods) have much longer engagements in the new design, and the results of the gap control study in Section 2.6.2 above indicate that this should not be an issue here.



**Figure 2.6.4-3:** Drawing the module back until it is seated in the FPSP

In Figure 2.6.4-4, the installation tool has been removed and a temporary locking collar installed on one rod (shown here on the upper one) to keep the module in place. The mounting screw and spring are shown here, having been installed into the threaded holes in the end of the alignment pins until the head of the shoulders seat on the end of the pins. The springs apply force between the screw head and the FPSP, pulling the module against the plate with the amount of force determined in Section 2.6.3 above. Note that the slotted hole in the FPSP was chosen to be associated with the smaller of the two pin sizes in order to maximize the contact area for its spring.



**Figure 2.6.4-4:** Installation rod locking collar temporarily in place and mounting screws and springs installed

During screw installation, the spring's free height of 15 mm is slightly longer than the 13.8 mm screw length. The spring will therefore slightly aid in centering the screw over the mounting pin, and the oversized chamfer on the end of the screw will further help centering. It should be noted that development of a special tool to aid in screw installation could be beneficial. Such a tool might hold the screw (with its spring in place) by its head and have a hex bit to turn the screw.

Figure 2.6.4-5 below shows the setup after the loading rods have been unscrewed and withdrawn.

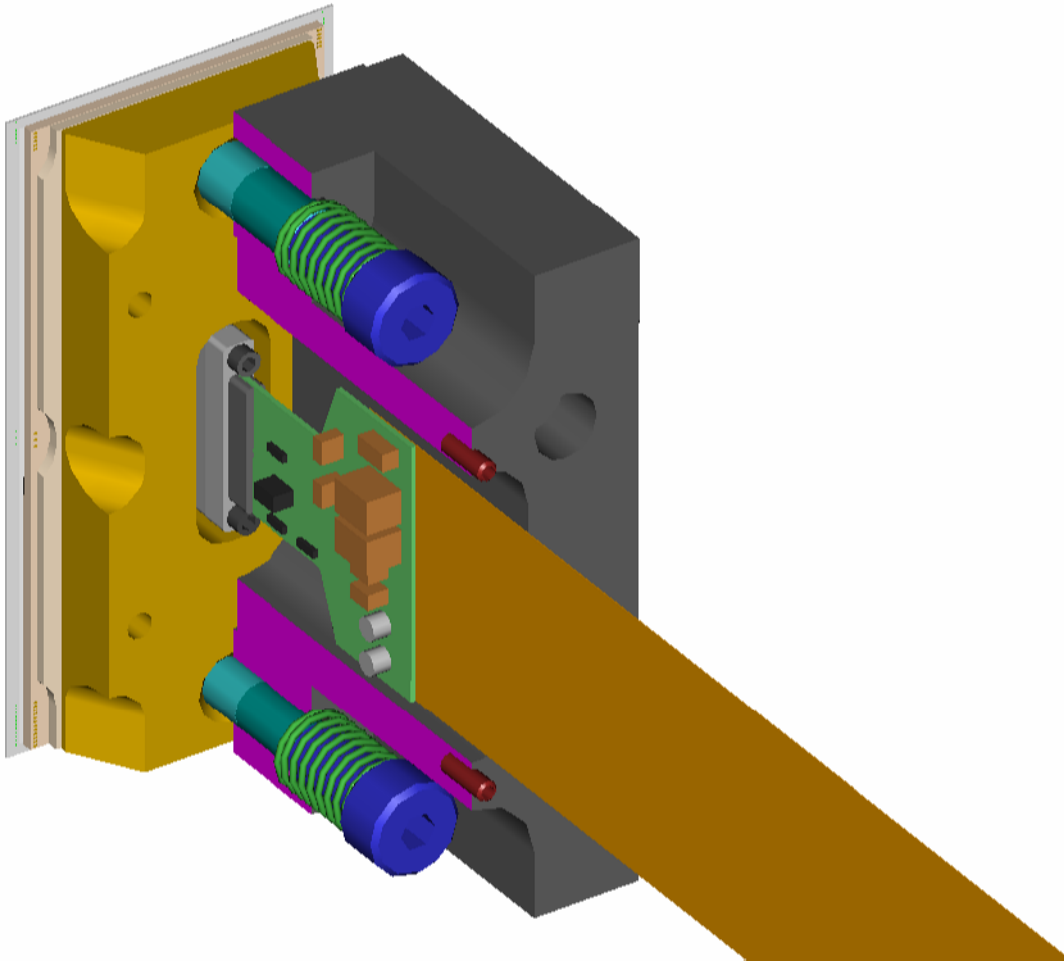


**Figure 2.6.4-5:** Module after installation rod removal

The cable restraint plate is shown in Figure 2.6.4-6 being installed over the cable. This is envisioned as having a thin slot slightly wider than the cable thickness and being relatively thick (slot depth shown is 6.35 mm) in order to constrain the cable's angle here but not its position along its length. The plate has holes that engage the small FPSP pins on either side of the cable clearance hole to set its position. It also has threaded holes into which are threaded panel screws. These screws have their threads machined off except for a short length near their ends. They are threaded into the plate here and therefore are not free to fall out and cause trouble.

Of course, if the electrical design determines that separate micro-coax cables are needed to run along with the flex cable, the configuration of this plate will be impacted, and the design of this part is therefore considered to be preliminary.

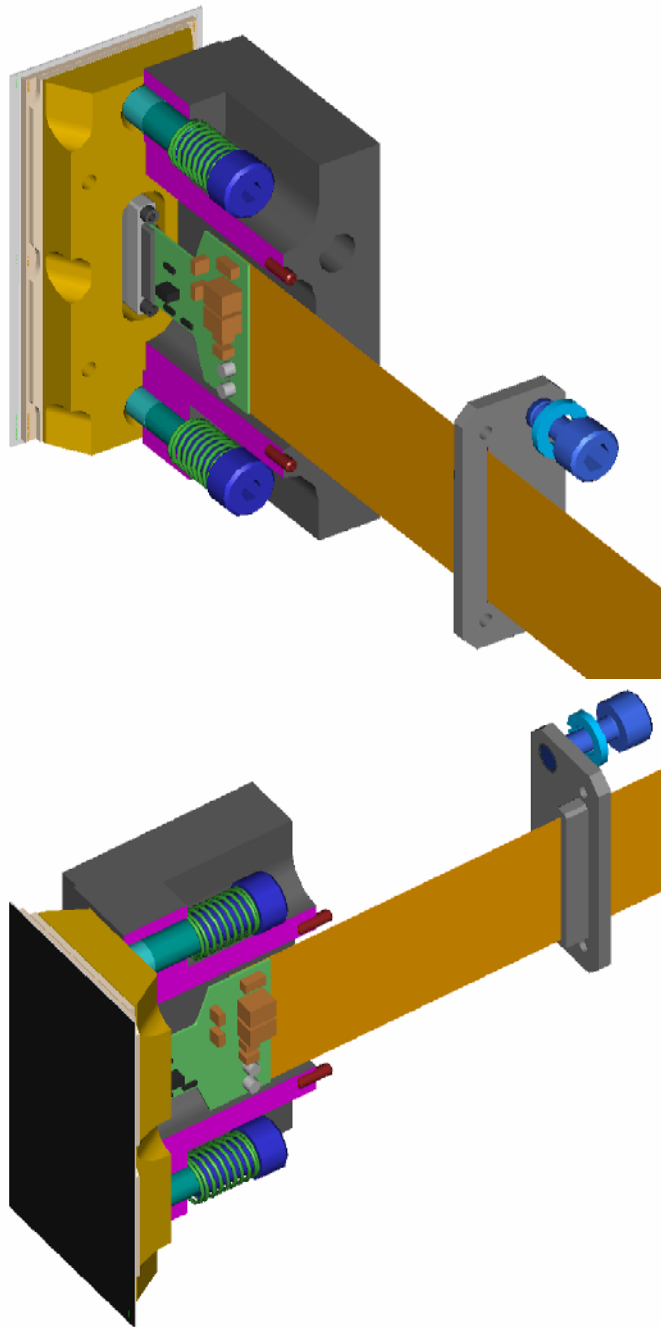


**Figure 2.6.4-6:** Sliding on the cable restraint (viewed from two different directions)

Figure 2.6.4-7 below shows the restraint plate installed on the FPSP. After it is seated in position on its pins, its mounting screws can be engaged. After a few turns, the threaded tip of each panel screw disengages from the threads in the restraint plate and jumps to the bottom of the counterbore in the FPSP, where further turning screws it into the threads machined into a portion of the loading rod holes. Lock washers maintain screw preload (and vent an otherwise trapped air volume). Then removing one of these plates for CCD replacement, the panel screws can be unscrewed from the FPSP but will remain captured by the cable restraint plate so there is no danger that they will fall out and potentially cause damage.

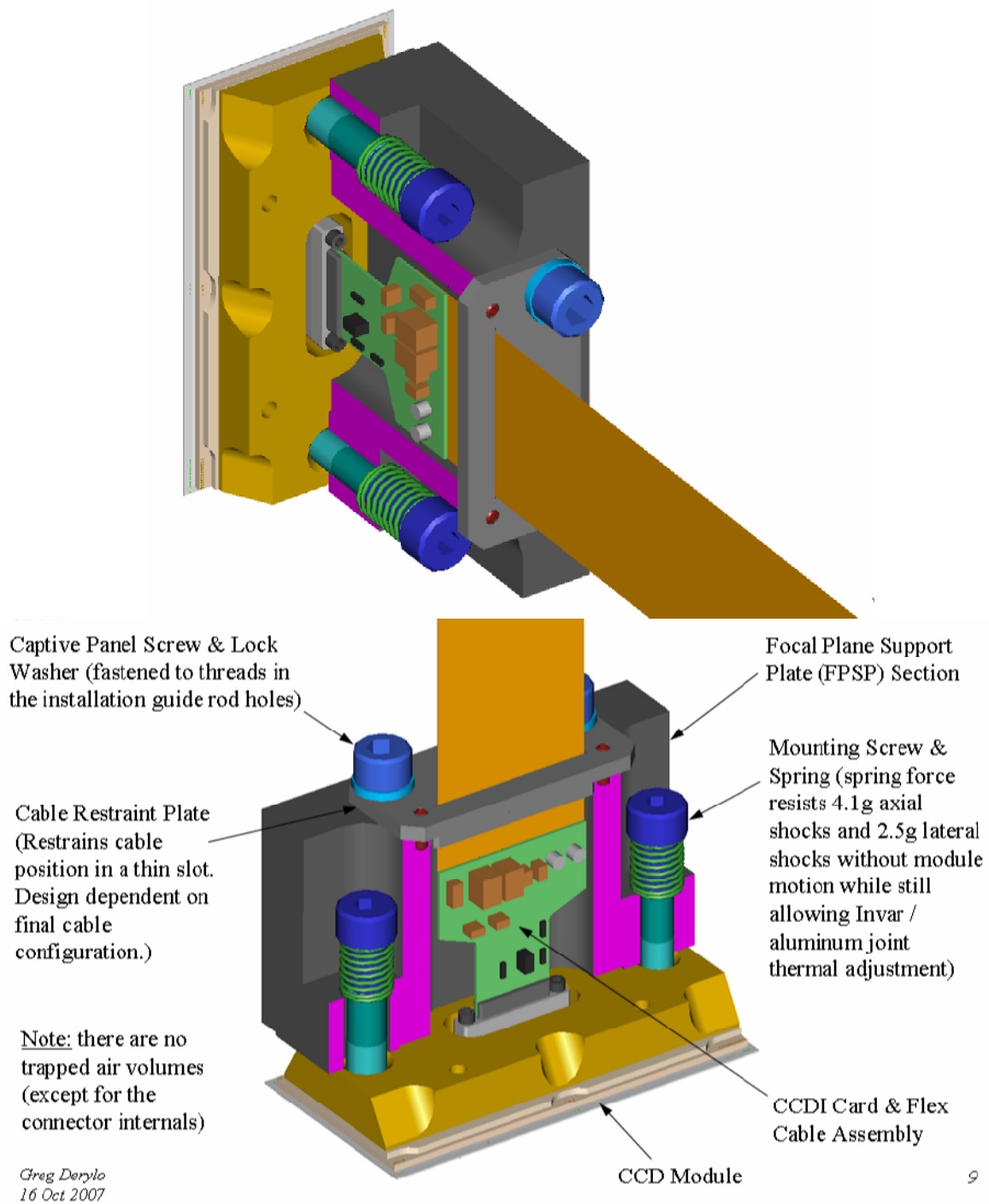


**Figure 2.6.4-7:** Installed configuration

As mentioned above, replacement of a module at CTIO must be considered. Some portion of the array will have to be uncabled from the VIB in order to provide access in the rear. Determining the necessary extent of this uncabling should be included as part of the effort to develop an installation sequence plan. Once the area is clear, a reverse of the procedure described above is envisioned for CCD removal. Again, two people, working from both the front and rear of the vessel, are necessary for this task.

## **2.7 MODULE STORAGE BOX**

The V1 storage box concept was extended for V2.0 to allow the box to be mounted, with its CCDI/cable assembly, in an ESD-safe storage container that was then stored in a shielded ESD-safe bag. The V2.0 box assembly is shown in FNAL drawing 436328.

Unfortunately, not enough experience was gained with this approach during the V2.0 effort. Further study of this concept should be included in the tooling design phase to evaluate the effectiveness of this layout.

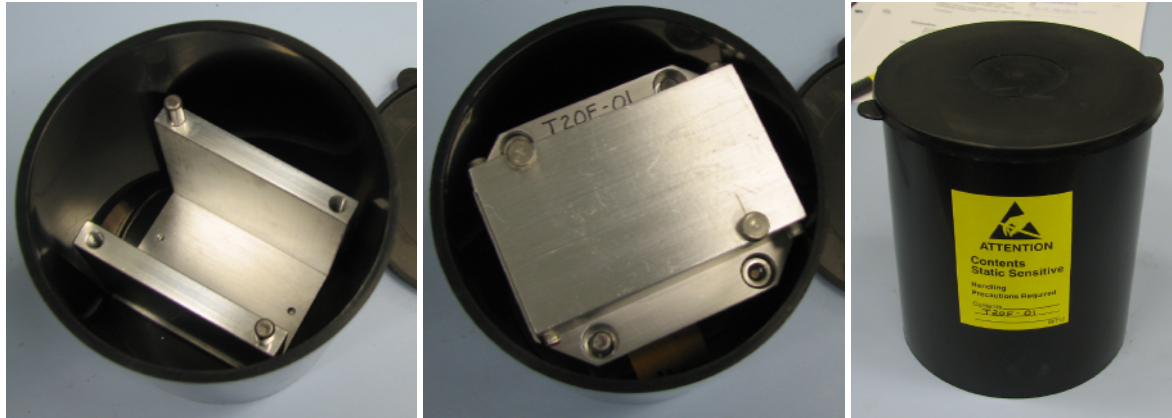


**Figure 2.6-1:** Storage Box and Container Constructed for V2.0 Modules

## **3.0 CONCLUSIONS**

The updated design of the 2k x 4k pedestal-style module has been presented. The assembly process is outlined and the manpower needed is estimated for a production rate of five modules per week. The results of FEA analyses are reported and found a  $\sim 3^{\circ}\text{C}$  gradient through the module and  $\sim 3.5$  microns of thermal distortion. Module mating with a revised FPSP design is discussed; including pin fit determination, module-to-module gap control, and spring load determination. An installation process concept has also been presented.

The new design is expected to provide an improved assembly process and hopefully an improved yield. The design's performance criteria are expected to be satisfied.

#### **4.0 REFERENCES**

1. MD-ENG-067, "Prototype Science CCD Module Design," by Greg Derylo, 1/20/05.
2. MD-ENG-110, "Updated Thermal Study of the DES 2k x 4k CCD Module V1 Design," by Greg Derylo, 9/5/06 [DES docDB #173].
3. Greg Derylo, H. Thomas Diehl, Juan Estrada, "0.25mm-Thick CCD Packaging for the Dark Energy Survey Camera Array", Proceedings of SPIE 6276, 2006.
4. MD-ENG-125, "DES 2k x 4k V1 CCD Module Flatness, Thickness, & Edge Alignment Results," by Greg Derylo, 6/26/07 [DES docDB #67]
5. DES docDB #467, CD-1 Review CCD Packaging Breakout Slides, by Greg Derylo, 5/1/07.
6. DES docDB #979, V2.1 2k x 4k CCD Module Drawings & Design Report (this report!).
7. DES docDB #104, CCD Packaging Procedures & Travelers.
8. DES docDB #664, Test of "First Contact" Cleaning Polymer on CCD Surface.
9. DES docDB #806, "Dark Energy Camera Specifications and Technical Requirements, Version 1.0 (proposed)", by Tim Abbot et.al, 10/12/07.
10. DES docDB #763, "Environmental Conditions at DES Sites," 8/29/07.